Millimeter wave traveling wave tubes for the 21st Century

Claudio Paoloni[a], Diana Gamzina [b], Rosa Letizia [a], Yuan Zhang [c],

Neville C. Luhmann, Jr. [c]

[a] Engineering Department, Lancaster University, Lancaster, UK
[b]SLAC National Accelerator Laboratory, USA
[c]Dept. of Elect. Eng., Univ. of California, Davis, USA

Corresponding author

Claudio Paoloni, Engineering Department, Lancaster University, Gillow Avenue, LA1 4YW, Lancaster, UK email :c.paoloni@lancaster.ac.uk

Acknowledgements

The work has received funding from the European Union's Horizon 2020 research and innovation programs under grant agreement no 762119, from EPSRC DLINK - D-band Wireless Link with Fibre Data Rate grant EP/S009620/1 in the UK, and from DOE DE-FG02-99ER54518 and DE-FG02-99ER54531 in the US.

INVITED REVIEW ARTICLE

Millimeter Wave Traveling Wave Tubes for the 21st Century

Keywords: Traveling Wave Tubes; millimeter waves, backward wave oscillators, vacuum electronics,

Abstract

Traveling wave tubes are rapidly evolving to provide unprecedented power level in comparison to solid state devices in the millimeter waves region of the spectrum (80 – 300 GHz) thus enabling a wide range of applications.

Wireless communications, imaging, security, plasma diagnostics, healthcare and many others will gain substantial features if high power in the millimeter wave region would be available from compact sources.

The development of fabrication technologies is proving crucial for introducing new topologies and structures for millimeter wave vacuum electronic devices, compatible with the dimensions dictated by the short wavelength that poses substantial challenges due to tight tolerances and surface quality.

This review paper will provide an overview of the principles, evolution and state of the art of one of the most widely utilized vacuum electronic devices, the traveling wave tube (TWT). The wide band, high gain features of TWTs make those devices the most promising solutions for high power at millimeter waves and THz frequencies.

Introduction

Microwave vacuum electron devices or microwave "tubes" utilize free electrons in a vacuum to convert energy from a dc power source to an RF signal. There exist a wide variety of microwave tubes including triodes, linear beam devices, crossed field devices, periodic beam devices, gyro devices, forward wave devices, and backward wave devices,

as well as fast wave and slow wave devices. In the following, these terms will be briefly explained with the reader referred to the references for more details [1-5]. Most microwave vacuum tubes fit into more than one of these categories.

The energy conversion or "interaction" process differs markedly among microwave tubes. However, explanations of the various interactions all employ one or more of the following terms: electron bunching, linear velocity modulation, angular velocity modulation, and phase focusing [6]. Bunching refers to creating higher density groups of electrons as in triode vacuum tubes [1]. Linear velocity modulation refers to changing the electron energy along the propagation direction of the electron beam as in a linear beam device while angular velocity modulation refers to changing the energy of electrons azimuthally in a plane perpendicular to a steady magnetic field as in gyro-devices. Phase focusing refers to increasing or decreasing the coupling of electrons according to their positions and drifts as in M-type (crossed field) devices and peniotrons.

In linear beam devices, electrons amplify rf fields through loss of kinetic energy. In these devices, an electron stream, formed and accelerated by an electron gun, is injected into an interaction region. Here, while drifting in relatively rectilinear motion, the electrons form bunches in the retarding field of a wave which is on, or inside, a nearby structure. As the electrons give up energy, the rf wave amplitude increases.

Perhaps the most successful microwave and millimeter wave amplifier has been the traveling wave tube (TWT). In traveling-wave tubes (TWTs), the electron stream moves in the field of a traveling electromagnetic wave whose phase velocity is slowed to the beam velocity by e.g. helices, coupled cavities, or ring bar and ring loop. When the velocities are approximately equal, the rf wave amplifies.

The paper aims to be a comprehensive review of the state of the art of millimeter wave TWTs, with a mention to Backward Wave Oscillators (BWOs) that belongs to the TWT family.

The paper starts with the description of the main applications of TWTs followed from an overview on the working mechanisms. The historical evolution of TWTs from helix to more advanced configuration is introduces. A section on advanced fabrication technology will inform on the fabrication challenges of millimeter wave TWT. Finally, a review of the main interaction structures will be proposed, supported by the most interesting examples of fabricated millimeter wave TWTs.

1 TWT applications

Although the TWT was invented by Kompfner in 1942, this device remains an integral constituent of satellite communication systems, electronic countermeasures, and radar systems [7-11]. The success of TWTs can be attributed to their wide instantaneous bandwidth (greater than three octaves have been achieved in some devices), high gain (up to 70 dB), and light weight (typically 2-200 lbs.). Operating frequencies are typically from 1- 200 GHz with pulsed power levels in the 0.1-3 MW range (nominal 10% duty) and CW levels in the 10 W - 20 kW range. As noted later, modern fabrication techniques have extended their operating frequency regime to 1 THz.

The output power TWTs can provide is at least one or two orders of magnitude higher than any existing solid state power amplifier. This makes TWTs the enabling devices for a number of fundamental applications, mentioned above. So far, TWTs at frequency higher than 90 GHz are not yet in the market, but their availability will permit a number of new applications.

Transmitters in satellite communications systems are mostly powered by TWTs. In addition to the high power, TWTs are relatively unaffected by radiation and harsh thermal

conditions, making them highly reliable as required in the space environment. Currently, the maximum operating frequency for space TWTs is about 70 GHz. However, it is already envisaged the use of E-band (71 – 86 GHz) band for very high data rate satellite communications [12].

The use of TWTs in wireless communications is gaining interest for the opportunity to exploit the spectrum above 90 GHz. More than 100 GHz bandwidth is available between 90 GHz and 300 GHz. This permits 10s gigabit per second data rate. The main obstacle for the use of this frequency range is the high atmospheric and rain attenuation and the available transmission power of millimeter solid state devices that limits the transmission range to very short distance or needs very high gain antennas, with significant difficulty of alignment and sway. The development of wireless systems based on the use of TWTs are in progress for enabling point-to-multipoint, multigigabit per second data distribution that will provide an affordable replacement of fiber over wide areas, with substantial cost reduction.

Plasma diagnostics of microturbulence in nuclear fusion reactors is an application that would benefit from the availability of high power THz sources. The nonperturbative diagnostic is based on collective Thompson scattering. So far, only bulky and low power laser sources are available. Backward wave oscillators are the ideal radiation source for this application. An international collaboration is working to produce a 0.346 THz BWO [13].

A possible application of TWTs is in imaging. The wide band and high power at millimeter waves permit high resolution and stand-off imaging. A novel application where TWTs are pivotal is the ViSAR (Video Synthetic Aperture Radar) at 235 GHz [15]. It is able to penetrate clouds and works in all-weather conditions providing high

resolution imaging. A TWT with 50 W of average power at long duty cycles across the entire band of operation is used [15].

TWTs are also the power amplifier of a wide range of electronic countermeasures, typically at frequency below 40 GHz.

TWTs are enabling amplifiers for well-established and future applications, making possible the exploitation of the millimeter wave spectrum.

Figure 1 shows the broad range of performance achievable by TWTs and other vacuum electron devices up to 300GHz. It demonstrates the relevance of TWTs as enabling devices for the applications described.

New fabrication tools and technology as well as modeling tools and new applications are fueling a renaissance in high frequency TWTs and BWOs.

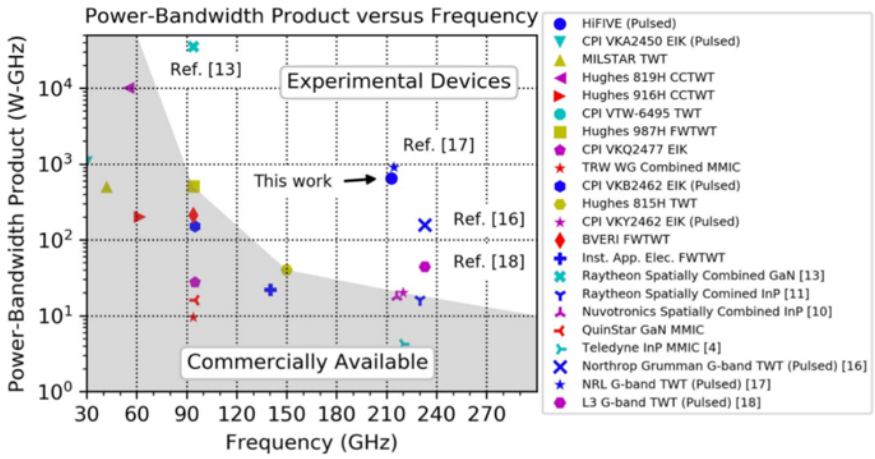

Figure 1 State of the art for TWT performance [87] (references in the figures can be found in the original paper)

2 - Physical Mechanisms of TWT Operation

A simple picture of TWT amplification is obtained by considering a group of electrons approaching a retarding field. The electrons will lose kinetic energy and gain potential

energy, thereby adding energy to the retarding field. If the electron density increases sufficiently during this process, the space charge fields also add to the retarding field. In a TWT, groups of electrons undergo similar energy changes in the retarding portion of an RF field traveling inside the device. This leads to amplification of the RF field.

To better understand the physical picture of the TWT interaction, consider Fig. 1. which illustrates the case of a wave propagating along a helix through which an electron beam is assumed to propagate. Although the wave propagates at essentially the speed of light along the helix, its effective forward velocity is sufficiently slow (as determined by the helix pitch) to synchronously interact with the electron beam traveling at $u_o \approx 0.1c$. Figure 1 also schematically illustrates the variation in the axial electric field strength of a continuous bunching process. Due to the negative charge of electrons, positive (negative) E_z results in a force to the left (right). This leads to bunching about the positions indicated by B in Fig. 2. This leads to a larger number of electrons in the region of the decelerating fields (position B) as compared to the accelerating field.

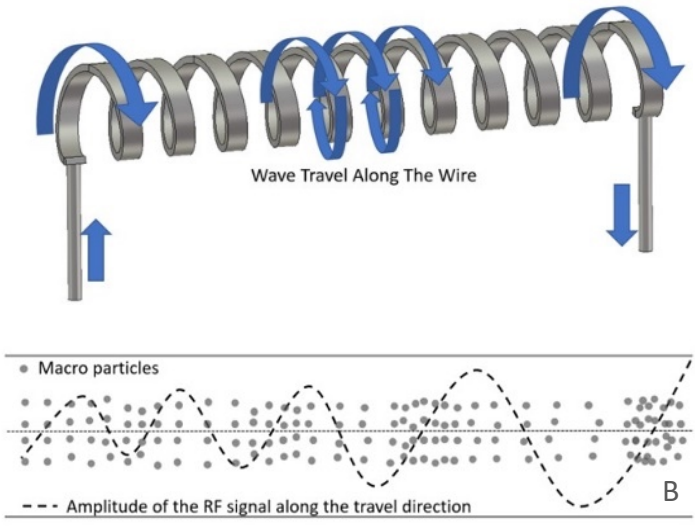

Fig. 2 Schematic illustration of the interaction between an electron beam and a wave propagating along a helix.

At the entrance to the helix, the electrons have a drift velocity slightly greater than the phase velocity of the rf wave and bunch near the nodes of the electric field. The electrons traveling through the helix continuously drift toward the decelerating electric field, causing an increase in wave amplitude. As the field amplitude increases, the bunching process becomes stronger leading to a reinforcement in wave amplitude and exponential growth below saturation.

As we shall see in the following, there are currently two major types of traveling wave tubes in active use: helix TWTs and coupled cavity TWTs, although a variety of other circuits such as folded waveguides, corrugated waveguide, ring-bar, grating, and ladder configurations are either employed in specialized applications or are under investigation for millimeter wave TWTs. [18 - 25] The former has essentially continuous interaction while the latter has interaction only in the cavity gaps. In all cases, the slow wave circuit has a phase velocity less than the velocity of light in order to synchronously interact with the electron beam and is a forward wave (phase and group velocity in the same direction as shown in Fig. 2). Figure 3 displays sketches of commonly employed slow wave circuits in commercial TWTs. The particular choice of SWS depends upon a number of criteria including operating frequency, bandwidth, peak and average output power, and gain. The broadest bandwidth is obtained with the helix SWS, particularly with the use of so-called "dispersion shaping" [26-27]. As it will discussed in the following, unfortunately, helix SWS cannot be used above 60 -70 GHz due to difficulty of fabrication.

The application of the above criteria to the tape helix structure reveals a number of its natural advantages. Perhaps the most important advantage of the helix structure lies in its broad bandwidth which is due to the low dispersion of the circuit. This property is essential to its use in communications and electronic countermeasures (ECM) applications as well as wide bandwidth laboratory amplifier usage.

Table 1 Representative performance characteristics of space TWTs				
Band	Output Power	Approx. Efficiency	Approx. Mass	Manufacturer
L-band (1- 2 GHz)	80-250 W	63-70 %	3,500 g	L-3
C-Band (4 – 8 GHz)	80-140 W	64-68 %	1,165 g	L-3
X-band (8 – 12 GHz)	100-160 W	64-69 %	1,250 g	L-3
Ku-band (12 – 18 GHz)	35-205 W	60-71 %	695 g	L-3
K-band (18 – 27 GHz)	150-300 W	63-68 %	1,400/1,700 g	L-3
K-band (18 – 27 GHz)	160 W	63 %	900 g	Thales
Ka-band (27 – 40 GHz) Q-band (33 – 60 GHz) V-band (40 – 75 GHz)	10-200 W	30-60 %	1,500 g	L-3
Q-band (33 – 60 GHz)	40 W	50 %	950 g	Thales

There are several reasons which lead to the power limitations of helix tubes. The small heat capacity of the structure provides a significant limitation on the power handling capability. However, there are additional constraints which should be understood. First, we must employ electron beams which only partially fill the helix tunnel in order to help suppress backward wave oscillations [17]. This, therefore, results in a limitation on beam current due to space charge forces for a given beam voltage. Simply increasing the beam voltage is not a viable solution since this requires that the helix pitch angle be increased to maintain synchronism. This results in a decrease in the interaction impedance for the forward mode thereby decreasing the efficiency. In addition, the relative impedance at the spatial harmonic is increased, thereby leading to increased susceptibility to backward wave oscillations. Consequently, most helix tubes have tended to operate with beam voltages of <10 kV. Although limited in power output capability, the helix TWT plays an important role in many applications, particularly telecommunications where the development history is reviewed in [7]. Table 1 displays typical parameters of helix TWTs used for satellite down-link applications.

Here, it should be noted that approximately 90 % of the world market is shared between L-3 Harris (US) and Thales (France).

An interesting usage of helix TWTs has been in the so-called microwave power module (MPM) and millimeter wave power module (MMPM) [30]. This hybrid device combines the best features of solid-state device technology with that of vacuum electron devices. Specifically, the MPM consists of a low noise, solid-state MMIC preamplifier, a TWT vacuum power tube booster, a solid-state equalizer, and integrated power conditioner (IPC). Here, the solid state device provides the low noise input and initial gain while the TWT provides the final 20 dB gain. The small size and light weight have facilitated numerous applications including drone based systems. The development of the approach has moved from the 2-18 GHz microwave region to the upper millimeter wave region up to G-band (230 GHz) [15]. Table 2 below displays the performance characteristics of most relevant MMPMs.

Table 2 Performance characteristics of MMPMs (from Ref. [15]).

	Ka Nano	Ka Band	Dual Ka/Q	Q Band	Multi-Band	E Band	Pulsed W Band	W Band	G Band
Freq	29-31 GHz	26-36 GHz	29.5-31 43.5-45.5 GHz	43.5-45.5 GHz	18-40 GHz	81-86 GHz	92-96 GHz	75-110 GHz	231-235 GHz
Output Power	50 W	100 W	80 W	80 W	100 W	100(sat)/ 50(lin) W	100(pk) W	50(min) W	rated
Volume	16.6 x 10.4 x 2.5 cm	24.1 x 20.3 x 3.8 cm	24.1 x 20.3 x 3.8 cm	24.1 x 20.3 x 3.8 cm	24.1 x 20.3 x 3.8 cm	364 in^3	410 in^3	364 in^3	364 in^3
Weight	1.1 kg	3.9 kg	3.9 kg	3.9 kg	3.9 kg	22 lbs.	23.5 lbs.	20lbs. max	20 lbs.

As mentioned in the preceding, the helix structure is not suitable for high power operation due to its limited heat dissipation capability. In addition, the high beam voltages required

for high power tube operation result in the evolution of the helix to a more open structure. Consequently, an increased fraction of the field energy is stored in high order spatial harmonics thereby degrading the interaction efficiency. The concomitant reduction in impedance and propensity toward backward wave oscillations lead to serious operating difficulties although some techniques such as the use of resonant loss have led to stable operation at increased beam voltage and power [31]. Using such techniques and modern computational tools, it has been possible to increase the operating voltage to ∼17–20 kV and the output power of K/Ka band and Q-band helix TWTs to the hundreds of watt level [32][33][34]. The above limitations motivated the development of so-called helix derived circuits (see Fig. 2) which partially ameliorate the situation, albeit at a cost in bandwidth among other problems. The ring-bar circuits tend to produce higher power (up to 200 kW peak and 10 kW average in UHF and L-Bands) with kW levels obtained at Ka-band [35]. Here, the phase velocities considerably exceed those of the simple tape helix with up to ≈ 0.4-0.5 c (where c is the velocity of light).

A related interaction structure is the Tunnel Ladder circuit [36][37] which grew out of the Karp Circuit [38][39] which is a ridged waveguide whose broad wall contains an array of transverse slots. In the baseband of this circuit, the electrons alternately see a strong field and a weak field as they pass, respectively, over a slot and over the metal between the slots, making spatial harmonic operation possible.

The concomitant reduction in impedance and propensity toward backward wave oscillations lead to serious operating difficulties for the tape helix TWT which were only partially ameliorated by the helix-derived circuits. This, therefore, led to the development of coupled cavity slow wave tubes shown schematically in Fig. 3 and which comprise the majority of current high power tubes despite their relatively narrow bandwidth. Basically, these can be thought of as derivations from series lumped LC element bandpass filters.

The coupled cavity structure possesses a number of attractive attributes. Of particular importance is the fact that the radial heat conduction is greatly facilitated by the metal webs which serve as the cavity walls. In addition, the shape of the structure is quite compatible with periodic permanent magnet (ppm) focusing and the assembly, although tedious, is relatively straightforward due to the symmetry. Finally, although inferior to the helix structure, coupled cavities provide moderate bandwidth (~ 2 - 30%) as well as reasonable interaction efficiencies and mode structure.

Coupled cavity TWTs (CCTWTs) have found service in the 1-100 GHz region with the lower limit set by the availability of alternative sources which are more cost effective. The upper limit is primarily set by machining and fabrication difficulties. As an example of the dimensions involved, the beam hole diameter in a 94 GHz tube is ~ 0.508 mm which is to be compared to the 0.1524 mm diameter of a human hair. Therefore, this necessitated the development of manufacturing processes which maintained tolerances of a few microns for the success of the early millimeter wave CCTWT developments. Bandwidths of coupled cavity tubes range from the order of a few percent up to ~ 43%. However, as we shall see, attaining bandwidths of even 30% requires a number of design compromises. Peak powers have ranged from ~ 100 W to 0.5-3 MW. The latter is not a hard limit and has resulted somewhat from the fact that the applications requiring high power have been able to be satisfied using narrowband amplifiers such as klystrons. Beam voltages have tended to be in the range of 8 kV to 85 kV. The lower limit arises because the cavity period decreases with decreasing beam voltage. The high frequency limitation arises both because the bandwidth decreases with increasing beam voltage and also because many applications preclude the use of high voltage. Finally, saturated tube gains up to ~ 60 dB are typical. This could be further increased, if necessary, by

increasing the number of gain sections from the present three to four although the possibility of external feedback induced oscillations would also be increased.

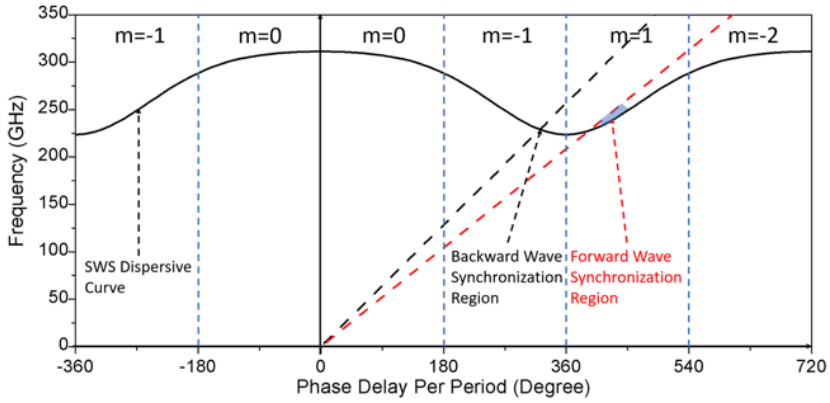

Fig. 3 Schematic illustration of the dispersion relation for a slow wave circuit.

The peak power limitation in coupled cavity tubes depends somewhat upon the space harmonic used for operation. Lower space harmonics require higher beam velocities to achieve synchronism and generate higher interaction efficiencies because of their higher interaction impedance. Since higher beam velocities also typically permit higher output powers, CCTWTs operating in a forward fundamental mode are found to produce powers about an order of magnitude above the peak powers from CCTWTs operating in a forward first-space-harmonic mode. At X-band, a 500 kW cloverleaf TWT [44] and a 1.2 MW centipede TWT [44] with high power, X-band tubes which produce between 100 to 125 kW (as also advertised in older sales brochures of Hughes Aircraft Co., Litton Industries, and Varian Associates). Table 3 displays the operating performance of representative currently available coupled cavity TWTs.

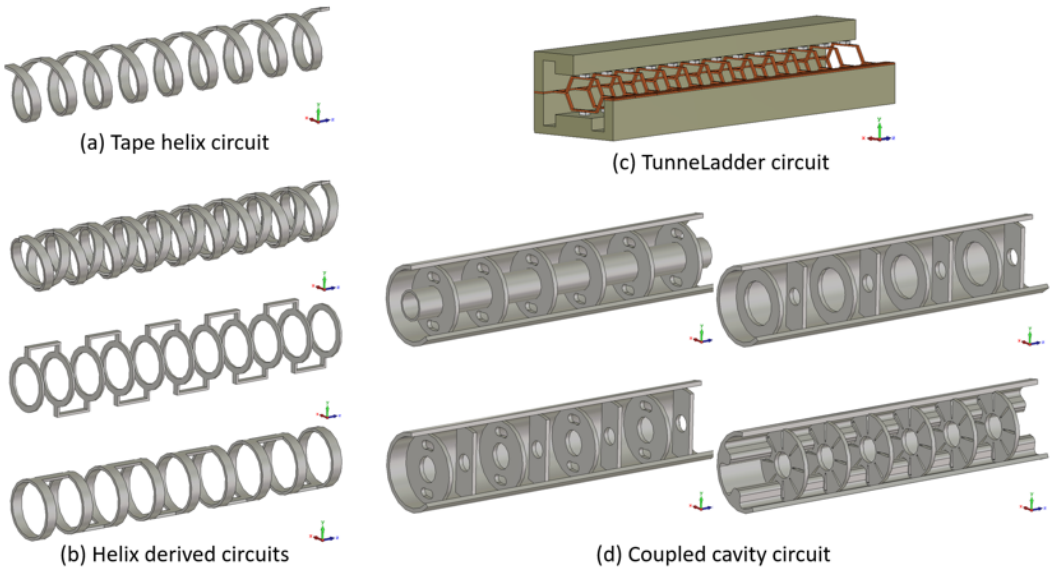

Fig. 3 Common commercial TWT slow wave circuits

Table 3 Operating characteristics of currently available coupled cavity TWTs.

Frequency Band	Operating Freq.	Power	Duty	Manufacturer
W-band	93-95 GHz	50 W	CW	CPI
W-band	95-96 GHz	3 kW	10 %	CPI
Ka-band	34.5-35.5 GHz	50 kW	30 %	CPI
Ka-band	30-31 GHz	500 W	CW	CPI
Ku-band	16-17 GHz	50 kW	0.3 %	L-3

2 Backward Wave Oscillators Operation and state of the art

Backward wave oscillators (BWOs) are similar to the TWTs discussed in the preceding section in that they employ a slow wave structure and a traveling wave interaction. However, they differ in one major respect. Specifically, the electrons interact with a

backward wave rather than a forward wave (see Fig. 3). As we shall see, this makes possible the operation of extremely broadband voltage tuned oscillators. A simple physical picture indicating the mechanisms responsible for the internal feedback of the BWO was developed by Heffner [24] and is illustrated in Fig. 5. Here, an electron beam is assumed to propagate at near the synchronous velocity close to the surface of a slow wave structure which supports a backward wave. The direction of phase advance of the wave is taken to be that of the electron beam propagation direction so that the energy flow on the circuit is opposite the beam drift. As with the TWT, the electric field of the circuit wave causes a velocity modulation of the beam electrons. Following a phase delay of π/2, this manifests itself as a current modulation which undergoes a phase delay of $\beta_e L$ as it travels a distance L equal to the circuit length. An additional phase delay of π/2 occurs as the current modulation excites the circuit electric field. Energy propagation along the circuit then undergoes a phase advance of βL due to the backward wave nature of the wave. In order to have feedback oscillations, one requires an integral multiple of 2π for the phase shift.

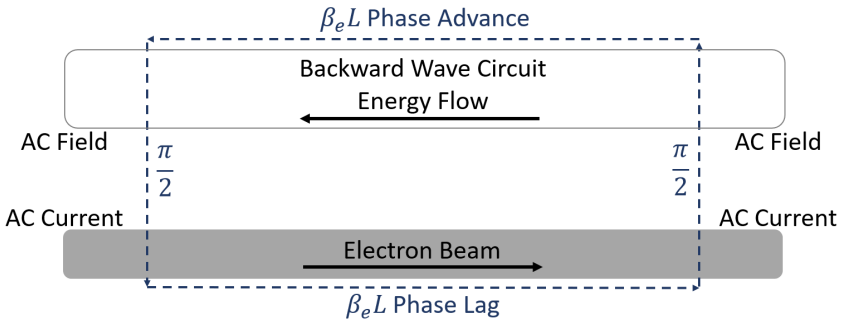

Fig. 5: The feedback loop of a backward-wave tube.

Historically, these devices have found extensive application as low to moderate power (≈ 1–300 mW) swept sources from the microwave to submillimeter wave region. There are both crossed field BWOs (sometimes referred to as M-type) and linear beam BWOs or O-type BWOs. Since the majority of the millimeter wave devices currently in use are of

the latter type, the discussion shall be primarily restricted to them. These are also sometimes referred to as carcinotrons which was the trade name for BWOs manufactured by Thomson – CSF (In December 2000, renamed Thales) . There are a number of excellent references concerning the principles of operation of BWOs as well as their design. The text by Gewartowski and Watson [1] provides a sound foundation for calculating BWO start oscillation and the connection to the TWT formalism described in the preceding subsection. Theoretical analyses of BWOs including start oscillation and efficiency calculations may be found in the papers by Heffner [24]; Johnson [25]; Grow and Watkins [26]; and Karp [27] . Construction details and performance data for some early BWOs operating in the 1-12 GHz region are provided in the paper by Palluel and Goldberger [43]. Information concerning millimeter wave BWOs can be found in the chapter by Kantorowicz and Palluel [46]. In addition, an excellent discussion of high power millimeter wave BWOs is contained in the chapter by Forster [47].

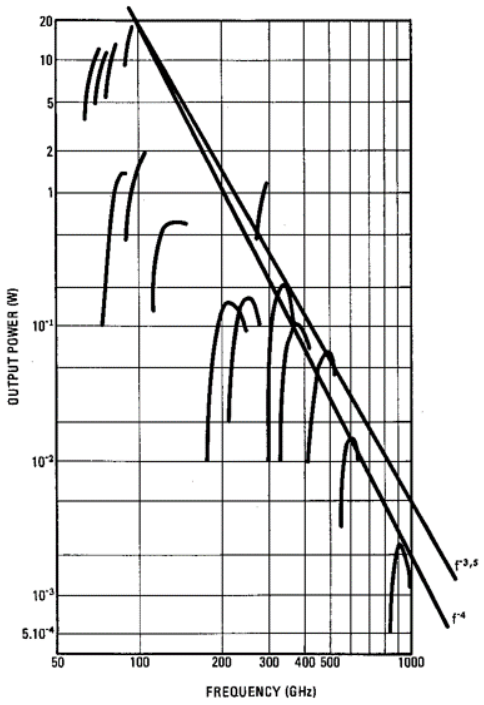

Fig. 6: Output power versus frequency for Thomson-CSF MMBWO family [48]

For many years, a major market for BWOs was in laboratory sweep oscillators up to 200 GHz. However, advances in solid state technology including active amplifiers and frequency multipliers have essentially eliminated that market. What remained was service as local oscillators in submillimeter wave astronomy, spectroscopy instruments, and as swept probe sources in plasma diagnostics [47] - [58].

Throughout the years up to 2000, the two main producers of BWOs were Thomson-CSF in France and Istok in Russia with tubes operating up to 1 THz, albeit at relatively low power (mW to W depending on frequency) with limited lifetime (200-2000 hrs.). The Thomson-CSF tubes employed a vane type circuit [43] [48][59]. The major problem with the vane type circuit is that the fundamental mode is a forward wave. The forward wave nature of the circuit necessitates operation with the first spatial harmonic with its attendant sharply reduced interaction impedance leading to higher required beam voltages and reduced efficiency. However, this shortcoming was in large part offset by the ease of machining fabrication and inspection for the vane structure. Figure 6 displays the output power versus operating frequency for the Thomson-CSF family of millimeter wave BWOs. Here, it is useful to review the features of the 1 THz tube which reveals the challenges and limitations also relevant for TWTs at the same frequency [48]. The vane type slow wave structure is shown in Fig. 7 for the 1 THz Carcinotron.

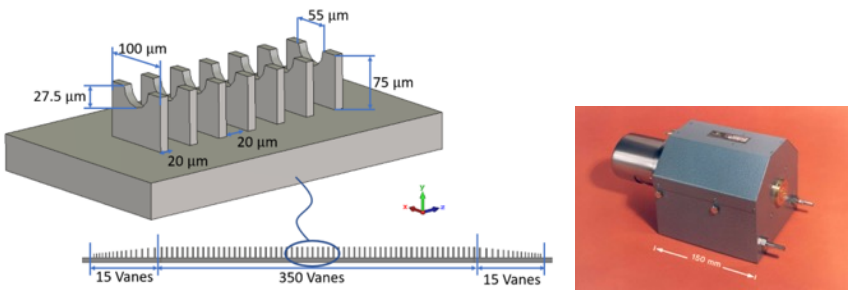

Fig. 7: Vane type slow wave structure for 850 – 1000 GHz Carcinotron [59]

The THz carcinotron employed the same basic fabrication and design techniques as their preceding tubes although severely pushing the limits of the technology of the time. This tube utilized a 500 μm diameter M-type cathode with the cathode emission densities potentially reaching 18 A/cm^2. However, some of the emission appeared to come from the edges and sidewall of the cathode thereby relaxing this number somewhat. Using an 8 kG $SmCO_3$ magnet system, the electron beam was compressed to 50 μm diameter for passage through the 55 μm beam slot shown in Fig.5. The cathode voltage was designed to vary between 4 to 10 kV over the operating frequency range of the tube. As shown in Fig. 7, the slow wave structure consisted of 350 vanes of uniform height with 15 vanes at both the input and output ends serving as matching sections. For comparison purposes, the lower frequency tubes had uniform sections of 200 vanes. The slow wave structure was milled out of copper using a 20 μm cutting wheel.

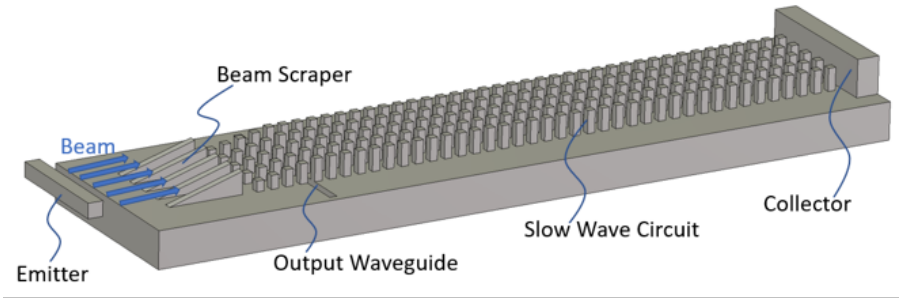

Fig. 8 Istok submillimeter wave BWO schematic.

THz BWOs were also developed by the Istok company in Russia and are still produced and sold [61]. As shown in Fig. 8, the approach differs from that adopted by Thomson-CSF. Here, instead of a circular cathode and large compression ratio, a rectangular cathode operating at high current density produces an electron beam which passes through a beam scraper which carves out the portion of the electron beam which would otherwise

impinge upon the fragile slow wave circuit pintles. In the simplest embodiment, there is no beam compression thereby requiring cathode current densities as high as possible consistent with acceptable, albeit limited, lifetime. Figure 9a displays the Istok submillimeter wave BWO performance characteristics with a photograph of the 900-1100 GHz shown in Fig. 9b.

Model	OB-65	OB-67	OB-80	OB-81	OB-82	OB-83	OB-84	OB-85
Frequency band, GHz	258-375	370-535	530-714	690-850	790-970	900-1100	1070-1200	1170-1400
Minimal output power, mW	1-10	1-5	1-5	1-5	0.5-3	0.5-3	0.5-2	0.5-2
Voltage, kV	1 - 4	1 - 4	2 - 6	2 - 6	2 - 6	2 - 6	2 - 6	2 - 6
Current, mA	25-40	25-40	30-45	30-45	30-45	30-45	30-45	30-45
Magnetic field, kOe	7	9	10	10	11	11	11	11

a)

b)

Fig. 9 a) Istok submillimeter wave BWO performance characteristics b) Photograph of Istok submillimeter wave BWO OB-83 (frequency band 900-1100 GHz, mass <250 g)

As noted in [61], the demand for, and hence development activity on, high frequency BWOs, similar statements apply to the Thomson-CSF carcinotrons, has significantly declined. This is attributable to the size and weight of the magnet, power consumption, lifetime, and the challenges in fabricating such tiny and delicate structures with the tools previously available.

Millimeter Wave and THz TWTs

The evolution from helix TWTs to new concept TWTs at millimeter waves is fostered by the use of new technologies and processes. The substantial amount of research and production of microwave TWTs described in the previous sections has been a fundamental stage for their evolution. The scope of this section is to describe the latest advancements in TWT technology.

Manufacturing processes have to respond to the accuracy and dimensions that the short wavelength at millimeter wave frequency require. Electron optics need a miniaturization approach to assure electron beams are of small diameter and well confined.

Slow wave structures (SWSs) have to assure the best beam-wave interaction with dimensions dictated by the wavelength and fabrication technologies. The most relevant millimeter wave SWSs and their implementation in TWTs, applicable also to BWOs, will be discussed.

Microfabrication technologies

One of the reasons for the slow development of mm-wave TWTs is the fabrication challenge that interaction or slow wave structures pose. The scaling down of dimensions at the increasing frequency brings the dimensions to the limit of conventional machining. High tolerance, extreme surface finishing, and flatness are only some of the parameters that have to be ensured for a high quality fabrication. As described in the following, most of the SWSs at millimeter waves have to be built in two halves, adding a further challenge in high precision alignment.

In the following, the principles of the most common microfabrication processes used for SWSs production are described. Further details can be found in the literature [62].

LIGA

LIGA is a German acronym for Lithographie, Galvanoformung, Abformung (Lithography, Electroplating, and Molding). It is a lithographic microfabrication process based on the use of thick photoresists (SU-8, PPMA, or KPRM) that produce high aspect ratio molds for growing copper structures by electroforming.

The LIGA process permits one to obtain sizes of features not achievable by CNC milling or other techniques, with high quality surface finishing.

Two different LIGA processes are available depending on the size of the minimum features: Deep X-ray LIGA (PPMA) and UV-LIGA (SU-8, KRPM) [64].

Deep X-ray LIGA uses metal masks and PMMA (Poly(methyl methacrylate) photoresist exposed to X-rays produced by a synchrotron light source. Aspect ratios up to 100:1 can be achieved. The first double corrugated waveguide at 1 THz realized by Deep X-ray LIGA is shown in Fig. 10 . The pillar section is 20*20 microns and the height is 60 microns [64]. The process is quite expensive and not widely available since it requires a synchrotron light source.

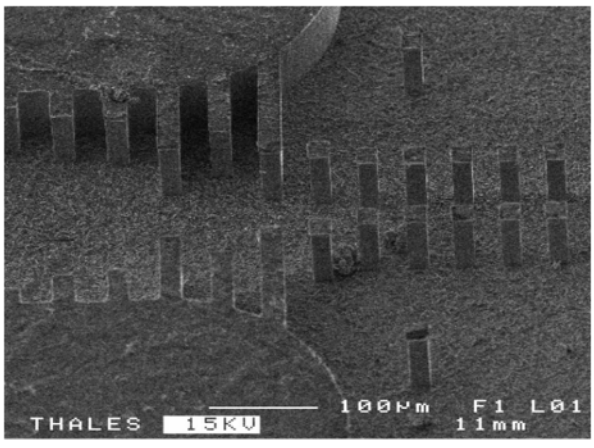

Fig. 10 Detail of DCW at 1THz realized by Deep X-ray LIGA. Pillar section is 20 x 20 microns, height 70 micron [64].

UV-LIGA, in contrast to Deep-X-ray LIGA, is an affordable process. The resist is exposed by an ultraviolet (UV) light available in normal mask aligners. Two different photoresists can be used, SU-8 and KMPR. SU-8, surely the most widely used for millimeter wave SWSs, provides higher quality molding, but it is very difficult to remove at the end of the process. KMPR is easier to remove, but it is limited in the achievable aspect-ratio . The maximum aspect ratio allowed by UV-LIGA is about 20:1, sufficient for most of the SWSs. Two examples of UV-LIGA SWSs are shown in Fig 11. Figure11a) shows a 1 THz folded waveguide [65] [66], while Fig. 11 b shows the pillars of a 300 GHz double corrugated waveguide [67] (the pillar section is 70x70 microns).

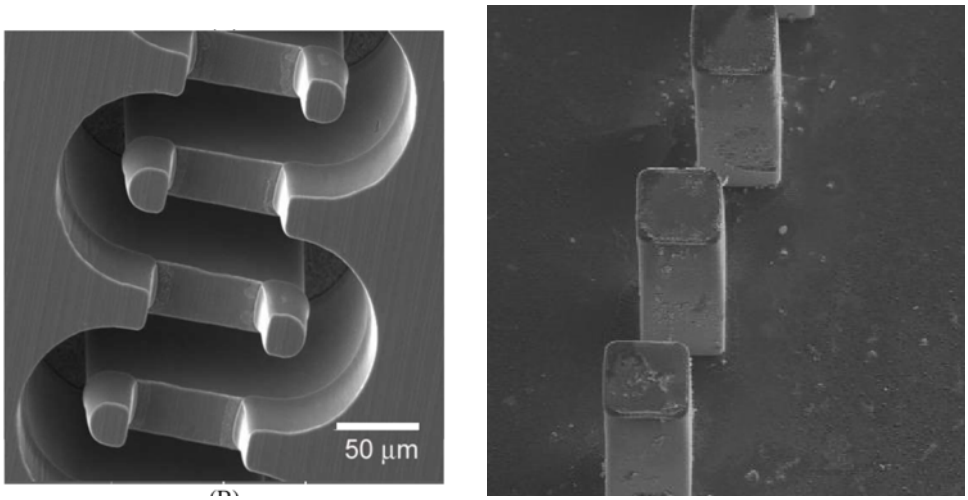

a) b)

Fig. 11 a) 0.67 THz folded waveguide [66]; b) 300 GHz double corrugated waveguide (pillars section 70x70 microns) [67].

Note the high quality of the metal surfaces. Other examples of LIGA fabrication are reported in [68] - [72] including the SU-8 removal process, and cold tests on different slow wave structures in the millimeter wave band.

High precision CNC milling

CNC (Computer Numerical Control) milling is the typical fabrication technique for metal parts. However, when the size of the features, as in millimeter wave SWS, approaches the 100 micron level and the surface roughness needs to be in the range of tens of nanometers, the process become very challenging and high end equipment is needed. The quality of fabrication is a function of the accuracy and resolution of the positioning and the availability of suitable toolings and high spindle speed (higher than 20,000 rpm) [79]-[87] . High-end CNC mills available in the market provide resolution of about 100 nm. At the top of the scale, there is the DMG Mori Seiki NN1000 developmental nano-CNC mill, available at the University of California Davis, that has a movement position accuracy of 1 nm/100 mm and a repeatability of 5 nm/100 mm. The spindle currently employed in the machine has a maximum speed of 50,000 r/min.

Tooling are of high importance for the size and the quality of the surfaces. The most suitable for high precision machining are coated carbide and diamond tooling. The minimum size available is 76 um diameter, that poses substantial material and use challenege.

Nano-CNC CNC milling has been demonstrated able to produce SWSs up to 0.346 THz (Fig. 12). The shown 0.346 THz double staggered grating structure is surely close to the limit of the CNC milling technology. It consists of two identical halves that have to be assembled with high precision alignment.

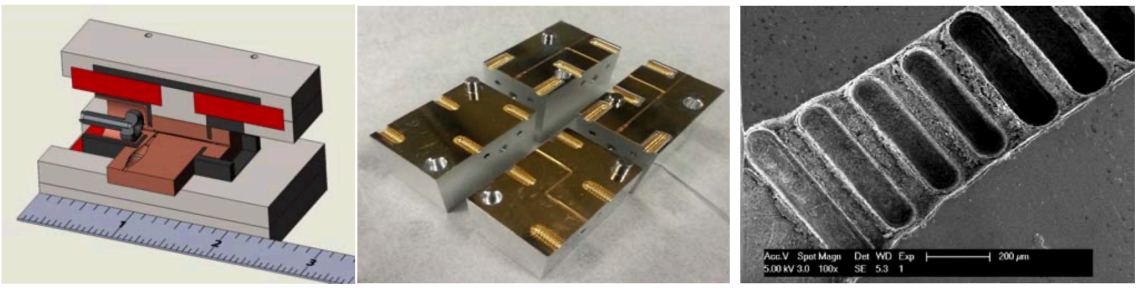

Fig. 12 Detail of 0.346 THz Double Staggered Grating (a) 346-GHz compact BWO shown with 6-in ruler for scale. (b) Cold test circuit structures. (c) SEM image of the DSG circuit cavities.

Commercial high end CNC milling is also used for SWS at lower frequency that do not need the level of accuracy above described.

Figure 13 shows two SWSs produced by a commercial high speed CNC milling (Primacon) with better than 1 micron accuracy. Figure 13 a) shows a 92 -95 GHz folded waveguide, specifically one of the two identical halves that once assembled formed the closed waveguide [84]. Fig. 13 b) shows a 140 GHz double corrugated waveguide [85].

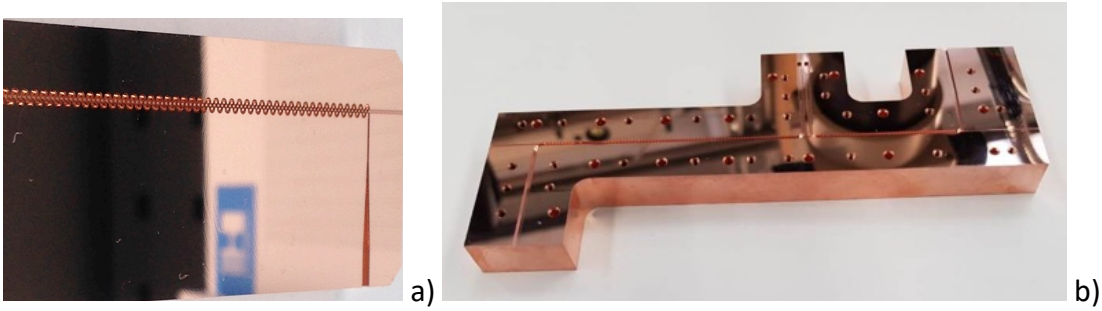

Fig. 13 a) High precision CNC milling a) W-band Folded Waveguide [84] and b) D-band double corrugated waveguide [85].

Micro Diffusion Bonding

The fabrication of the parts is the first step of the full fabrication process of a SWS. As mentioned above, millimeter wave SWSs are usually built in two halves to be assembled. The assembly has to be vacuum tight to maintain the high vacuum level needed for the functioning of the TWT (better than 10^{-8} Torr). Diffusion bonding is a process that

permits one to assemble two or more metal parts by rebuilding the atomic bonding at the contact surface [86]. This is achieved by applying a high pressure to the two halves to assemble by a specific holder. The holder is then baked at a temperature close to the melting point of the metal. The combination of temperature and pressure recreates the atomic bonding between the contact surfaces. The resulting bond is vacuum tight.

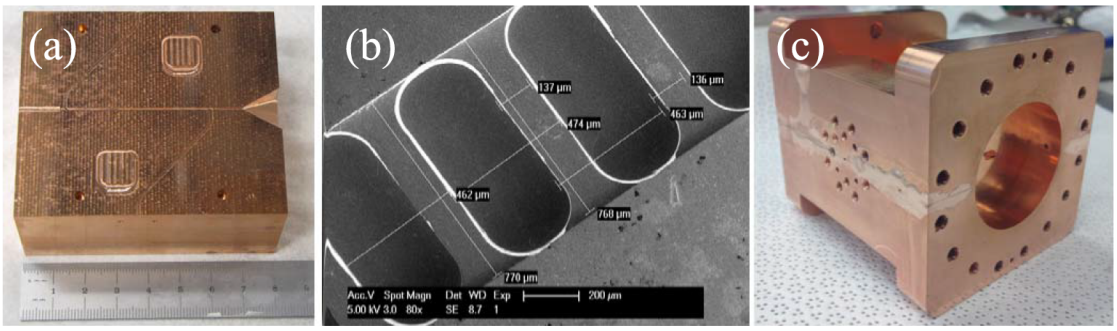

Fig. 14 Example of circuit blocks and diffusion bonding: 220-GHz DSG [83]

Electron Optics

The electron optics is the subsystem that permits the generation and collection of a confined electron beam with given shape and electrical parameters. The electron optics include the electron gun, the magnetic focusing system, and the collector. In this section, only the electron gun will be discussed since it is the most complex constituent of the electron optics and linked to the TWT performance. Details on the magnetic focusing system and collector can be found in literature.

The Pierce electron gun is the most used configuration, built to generate a cylindrical electron beam to interact with a helix SWS. It has been demonstrated to be suitable to

produce electron beams with 20 micron radius (Fig. 15) [64]. The focusing of cylindrical electron beams is well established by using periodic permanent magnet systems.

Recently, in response to the use of slow wave structure with a wide interaction field distribution, and the need to increase the current while maintaining a low current density, electron guns to produce electron beams with rectangular section (sheet electron beam) were realized (Fig.16).

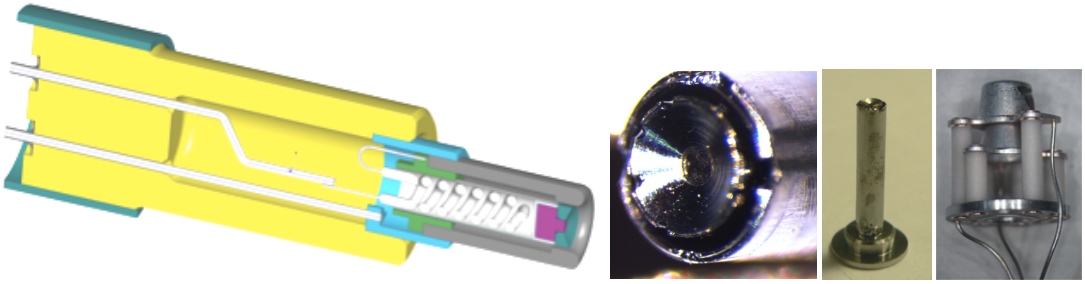

Fig. 15 Schematic and parts of an electron gun for 1 THz BWA [64].

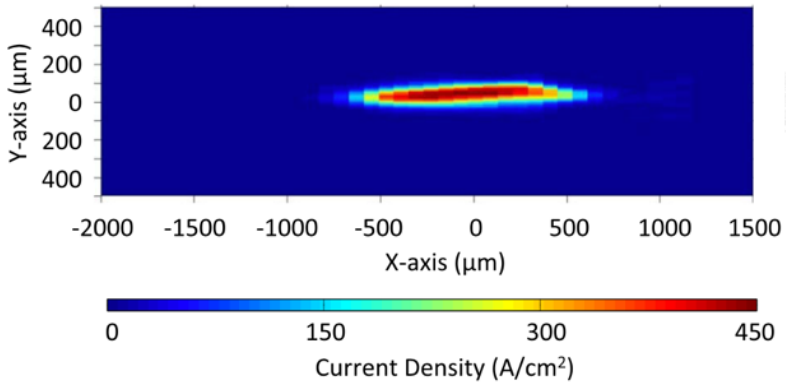

Fig. 16 Measured beam profile for with the nanoscale tungsten scandate cathode. The measured aspect ratio is 12.5:1, the maximum current density (dark red color on this plot) is 438 A/cm [87].

The advantage of sheet electron beams is their wider cross section that well matches the field distribution in corrugated "like" SWSs, usually distributed over a wide region closed to the corrugations. The main challenge of a sheet electron beam is to design the magnetic focusing system. Sheet beams suffer the diocotron $\vec{E} \times \vec{H}$ effect, that brings

a rotation of the beam and a critical level of impingement of electrons with the metal structure.

As the length of the beam transmission tunnel is increased, a periodic focusing magnetic field, rather than a uniform one, has been presented as a method to avoid kinking and filamentation instability [88]. Concurrently, by adopting a periodic permanent magnet (PPM) focusing system, the volume of the VED can shrink into the cm^3 range and the weight can be reduced to less than 10 pounds for THz frequency band operation. Previous work on this subject mainly focused on analytic studies to understand the interaction mechanism and theoretical modelling to design magnetic lens structures [89]–[90].

Several works related to the transport of gun-emitted sheet beams have been reported in recent years. An offset PCM structure developed by UC Davis has been employed in a W-band sheet beam klystron (WSBK) and the 90 A/cm^2 beam achieved 99 % transmission with RF [91] (Fig. 17). The focusing system for the WSBK is an offset periodic permanent magnet (PPM) which provides the appropriate vertical focusing force by periodic pole pieces and supplies the horizontal focusing force by the offset iron pieces.

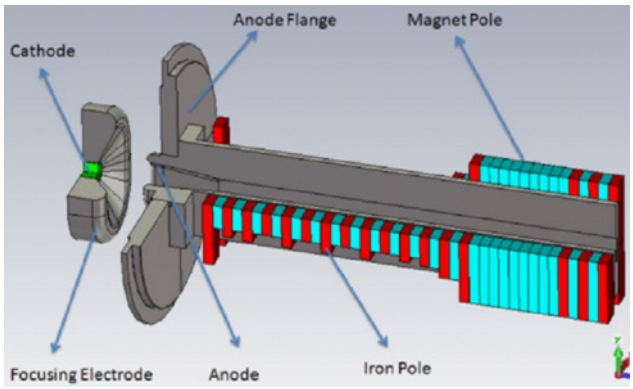

Fig. 17 W-band sheet beam klystron (WSBK)

The closed PCM focusing system adopts enclosed construction; it is rarely employed in high gain, moderate average power devices due to its restriction on space availability for the cooling channels of a liquid thermal management system. The traditional semi-open offset pole piece, periodic cusped magnetic (PCM) focusing system employed in W band tube sets the horizontal focusing magnet part at the fringe of the PCM poles. In addition, the width of the whole magnet is limited due to the requisite strength of the y-direction magnetic field. Consequently, the practical finite width of the traditional PCM will cause the tilt phenomenon in the beam mid-plane off the magnet array mid-plane which will deteriorate the beam transmission. A novel PCM-QM magnet has been presented to solve the abovementioned problems.

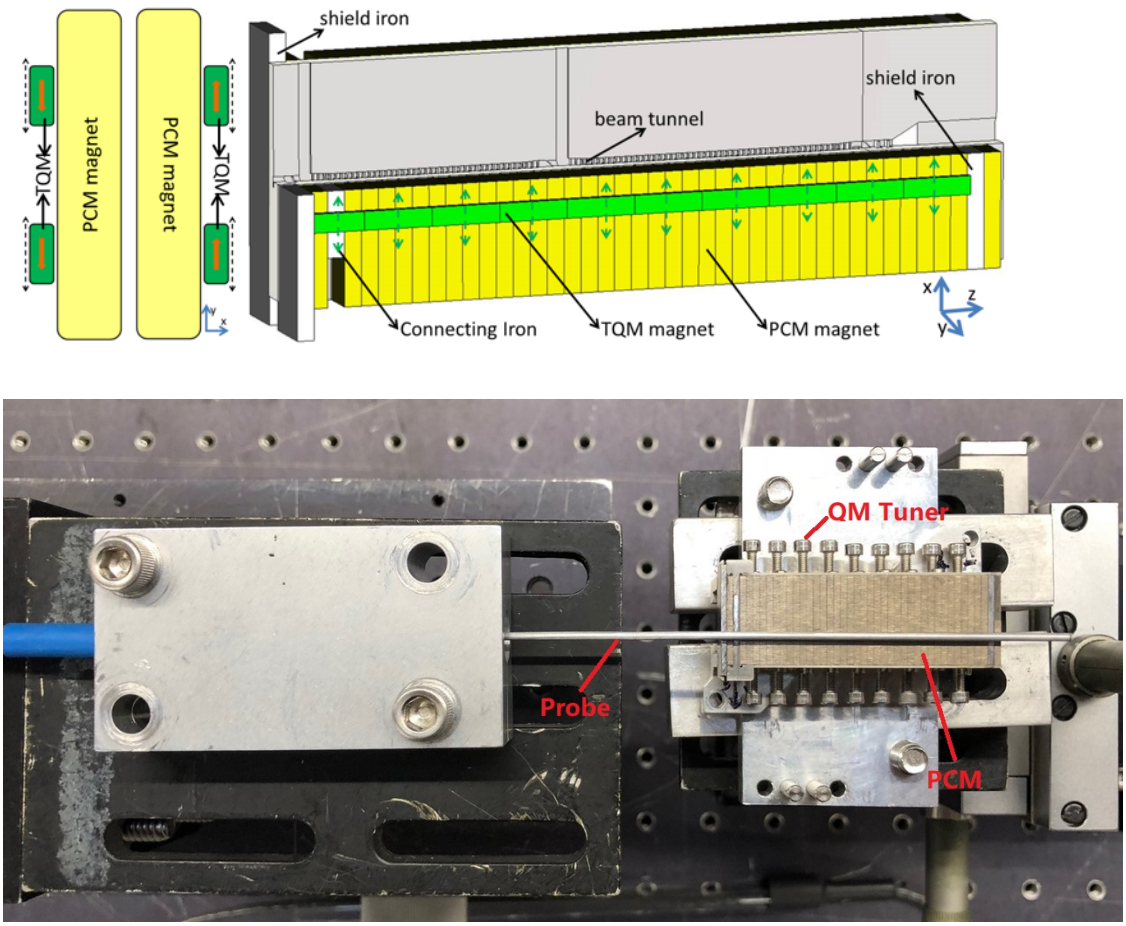

Fig. 18 transverse section and 3D beam transport model 220 GHz / 263 GHz SBTWT amplifier [92] schematic and fabrication.

Figure 18 shows the transverse section and 3D beam transport model, including the main circuit block and the novel PCM-TQM structure, of the prototype 220 GHz / 263 GHz SBTWT amplifier [92]. This hybrid PCM-TQM focusing system can provide vertical direction (y-z plane) focusing by the PCM part and, simultaneously, confine the horizontal plane dispersion tendency of the sheet beam by the independent TQM part. Compared with the traditional PCM focusing system, the PCM-TQM focusing system has several advantages: First of all, this kind of PCM-TQM eliminates the width limitation of the traditional PCM focusing system by placing the TQM poles on the top/bottom surface of the PCM part. Consequently, this kind of system can be compatible with a wider PCM part. Secondly, since the sheet beam gun is usually designed with different compression ratios in the vertical and horizontal planes, this can cause the vertical and horizontal beam waists to occur at different axial positions. This advanced PCM-TQM focusing system can produce magnetic focusing field matching of the vertical and horizontal beam transport separately, since the TQM is independent from the PCM part. Finally, each independent QM stack can provide adjustment capability by sliding on the top face of the PCM part along the broken line, shown in Fig.18, which can provide the PCM-TQM the ability to match the transversal focusing field with the varying beam current density. Furthermore, it provides the possibility of further adjustments to compensate for the inevitable magnet stack remanence variations and alignment issues after magnet assembly. Employing this PCM-TQM focusing system, the 263 GHz SBTWT achieves a 99.7% ‘no RF’ and a 97.6% ‘with RF’ beam transmission rate verified by CST-PS. Those results prove that this kind of structure has potential to benefit other sheet beam devices in the millimetre and sub-millimeter wave regimes.

Interaction structures for millimeter wave TWTs

Interaction structures or slow wave structures are the core of both TWTs, and similarly BWOs. They ensure the transfer of energy from the electron beam to the RF field. The quality of the energy transfer is measured by the interaction impedance [1].

As discussed, helix and coupled cavity [93] SWSs typically used at microwaves have high interaction impedance. However, when the frequency increases above 60 – 70 GHz, the fabrication of those interaction structures is not feasible. Different interaction structures suitable for millimeter wave TWTs have been conceived to be fabricated with by the technology processes described in the previous section.

In the following, the most interesting interaction structures for millimeter wave TWTs, the folded waveguide, the double staggered grating, and the double corrugated waveguide, will be described including their application in state-of-the-art TWTs. Other SWSs have been proposed, such as meander lines [94] - [101] or planar helices [102], but no TWT was so far designed to be built, so they will be not considered in the following.

Folded Waveguide

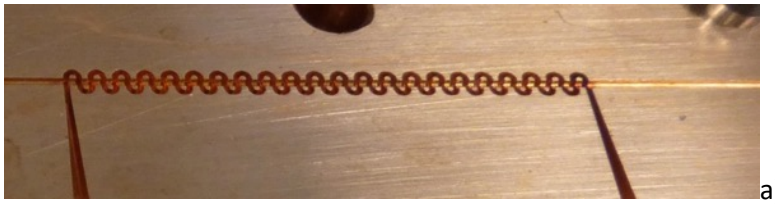

a)

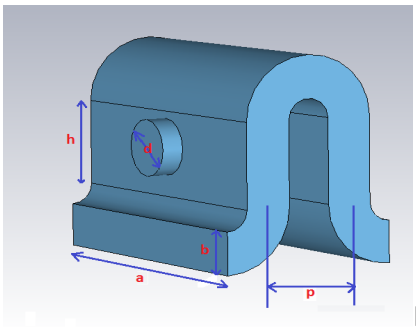

b)

Fig. 19 Folded Wave Guide SWS a) W-band copper sample, b) schematic

The folded waveguide (FWG) is a rectangular waveguide folded in a serpentine shape (Fig. 19a) to reduce the axial phase velocity of the EM wave to have synchronism with the electron beam [104]. The single cell of an FWG SWS is shown in Fig. 19b. It consists of a bent waveguide with a circular beam tunnel. Compared with the helix slow wave structure, the FWG has narrower bandwidth, lower interaction impedance, but can provide higher average power handling capability since it is a full metal structure. The coupler to the flange is very easy to design with very good matching. The equivalent circuit model of the FWG SWSs is comparatively simple and the reflection in the structure is small. The Pierce gain theory [16] is a good approximation to predict the gain feature of the FWG.

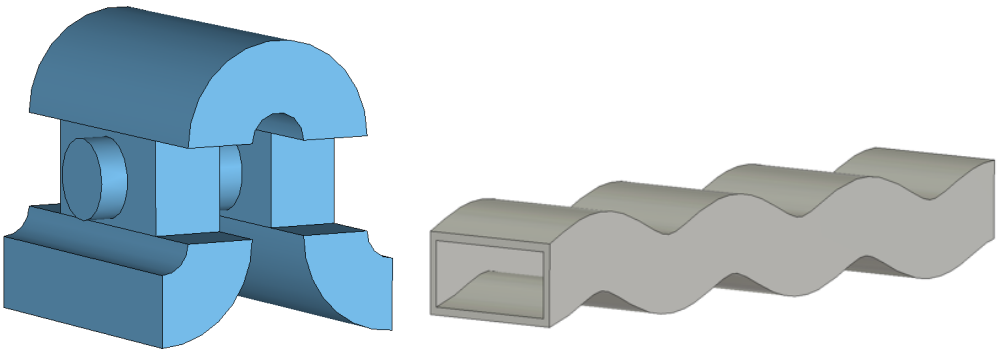

a) b)

Fig. 20 Modified FWG SWSs: a) ridge-loaded [105]; b) sine waveguide [112].

In the attempt to improve the interaction impedance, some modified types of FWG SWSs have been proposed, such as the ridge-loaded FWG SWS (Fig. 20) [105]-[110] . This topology has wider bandwidth, but also strengthens the longitudinal electric field thereby improving the electron efficiency of the beam-wave interaction. However, the complex geometric structure increases the manufacturing challenge at the increase of the frequency. To further simplify the fabrication of the FWG SWSs, and mitigate the ohmic losses, the Sine waveguide has been proposed for wideband, high-power terahertz TWTs (Fig.19 (b). It supports a sheet beam [112] - [115]. The interaction impedance of the sine waveguide SWS is low compared to a conventional FWG leading to a longer beam-wave interaction circuit, which will bring a challenge to the electron optical system.

Usually, an FWG is designed to work with beam voltage in the range of 10 – 20 kV. The Folded Waveguide is the most widely used among the SWSs at millimeter and sub-THz frequencies. This is due to the easy design, good coupling, wide band, and relatively high interaction impedance. However, the fabrication has to be done in two identical halves (both by LIGA and CNC milling) that are then bonded in a single block. The alignment of the two halves has to be highly accurate, otherwise the electromagnetic properties could be degraded. As an example (Fig.21), about 10 micron misalignment between the two halves (a) in a 92 - 95 GHz FWG generates a stop band at about 94 GHz (b), making the FWG not usable [84]. The improvement of the alignment accuracy permitted to remove the rejection band.

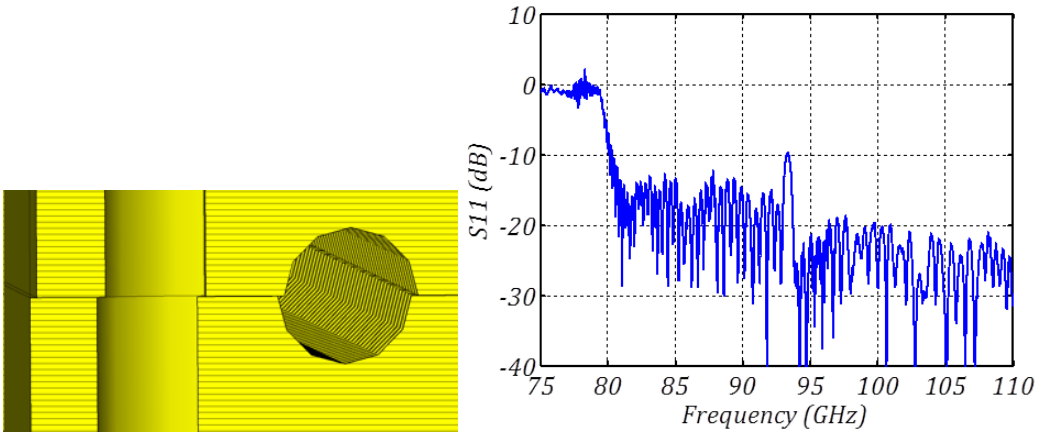

a) b)

Fig.21 94 GHz Folded waveguide: a) misalignment model; b) stop band due to misalignment.[84]

In the following, the most relevant FWG TWTs from 80 GHz to about 1 THz will be described, highlighting the variety of performance and approaches.

Folded waveguide TWTs below 100 GHz

Three FWG TWTs will be described below 100 GHz; some more were produced. A W-band (88 – 92 GHz) FWG TWT was presented in [73] with 38 dBm output power (Fig. 22).

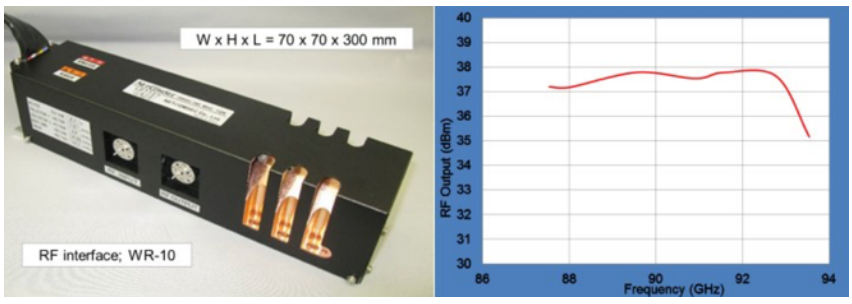

Fig. 22 W-band TWT: a) TWT, b) Output power [73]

A modified FWG, the ridge-loaded FWG, built by CNC milling (Fig. 23), was used for a

W-band TWT that produced 25 W over the 93.1 to 94.8 GHz band [105]. It is notable that output powers up to 100 W are reported, considering that solid state GaN PA can provide a few Watts for the most advanced amplifiers.

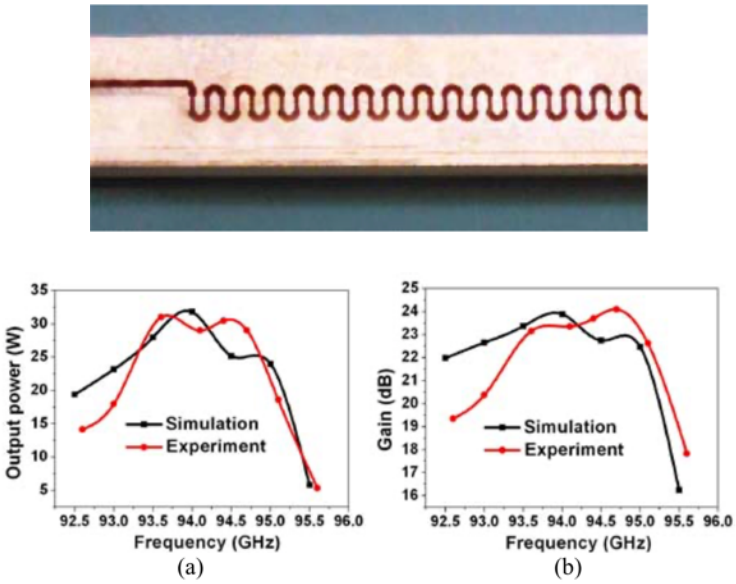

Fig.23 Ridge-loaded FWG, output power and gain [105]

A 91 – 101 GHz pulsed FWG TWTproduced 100 W output power with 6.7 GHz bandwidth and over 33 dB saturated gain at 20% duty cycle. The FWG was built by the LIGA process.

Folded waveguide TWTs in the range 100 – 220 GHz

The range above 100 GHz is gaining interest for wireless communications. A 140-GHz FWG TWT with an increased beam tunnel to improve the output power was reported

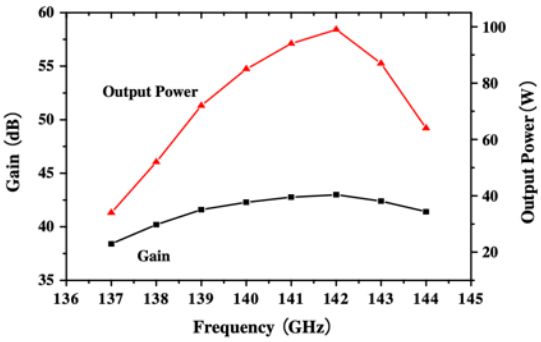

Fig.24 Simulated Gain and output power of 140 GHz FWG TWT with increased beam tunnel [117].

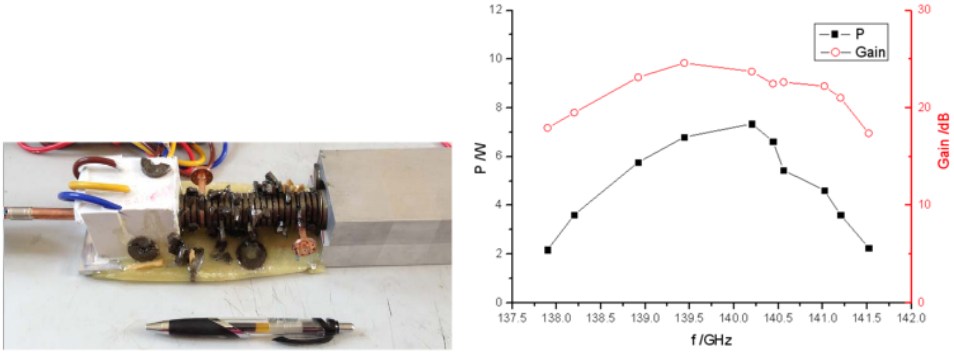

Fig. 25 a) Realized TWT, b) Gain and output power [119]

in [117]. The TWT was designed to produce more than 80 W output power (Fig. 24) . The first experimental prototype provided output power of 1.6 W with a gain of 25 dB.

A D-band FWG TWT with 7.3W, 25.3dB gain, and 3 GHz bandwidth at 140.3 GHz center frequency is reported in [119] (Fig. 25). The short length of the interaction section is noteworthy. The FWG was built by CNC machining.

To increase the power, a 220 GHz TWT was based on a folded waveguide circuit array with five FWGs coupled together (Fig.26a) to achieve about 180 W. It required a multi-beam (5) cathode and high aspect-ratio planar permanent magnet (Fig.26b) [77].

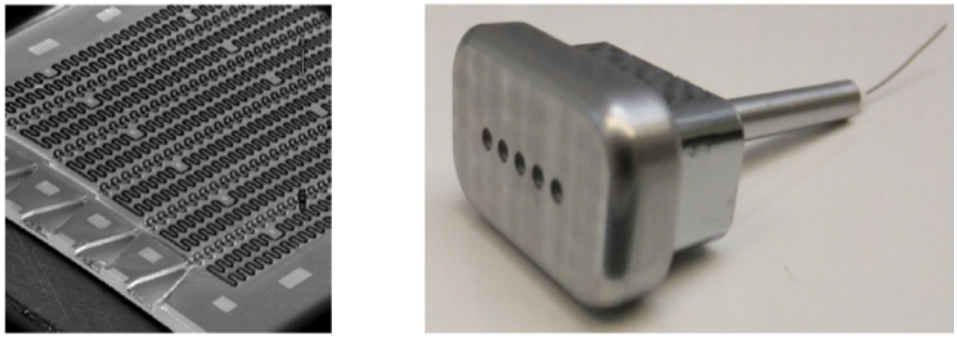

Fig. 26 a) 5-Folded waveguide circuit; b) 5 beam cathode and [77].

The UV-LIGA process was used to manufacture the FWG for 220-GHz TWT with 0.2 W output power in the band 212 - 221 GHz at 0.1% duty cycle (Fig. 27) [120].

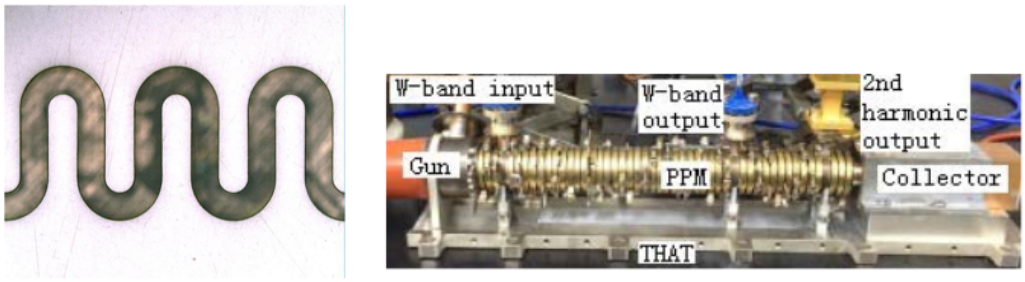

Fig 27 a) LIGA FWG, b) realized TWT [120]

A 220 GHz FWG TWT was presented in [121] with instantaneous 3 dB bandwidth of 8.8 GHz, and 350 mW peak power and about 16 dB gain (Fig.27). 15.7 kV beam voltage was used.

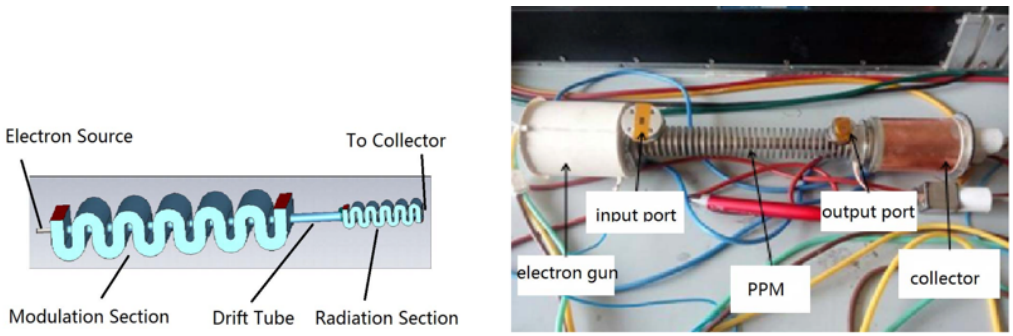

Fig. 28 a) FWG circuit with two sections at different frequency. B) realized TWT, the input flange at Q-band and the output flange at D-band. [122]

A different configuration of FWG TWT based on third harmonic amplification demonstrated 500 mW in the band 171.4 to 182.8 GHz (Fig. 28). The harmonic amplification is obtained by two sections of FWG. The first section amplifies the input signal at 43.5–45.5 GHz that is then multiplied by three by a second FWG section at 130.5–136.5 GHz [122].

Folded waveguide TWT above 220 GHz

Above 220 GHz, the most advanced configurations of FWG TWT were reported touching the threshold of 1 THz [118] - [124] . The fabrication of the FWG, due to the very short wavelength (below 1.5 mm) is mostly performed by LIGA. Some samples were built by CNC milling utilizing nano CNC milling and tooling in the range of 100-micron diameter.

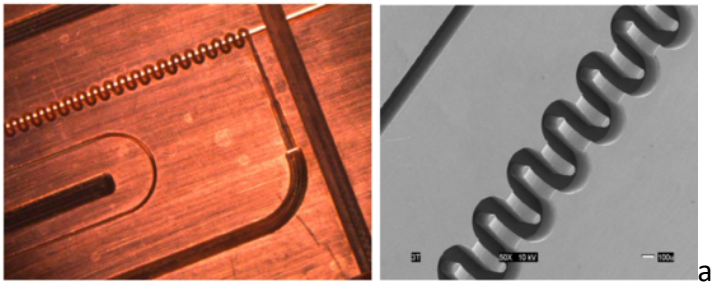
a)

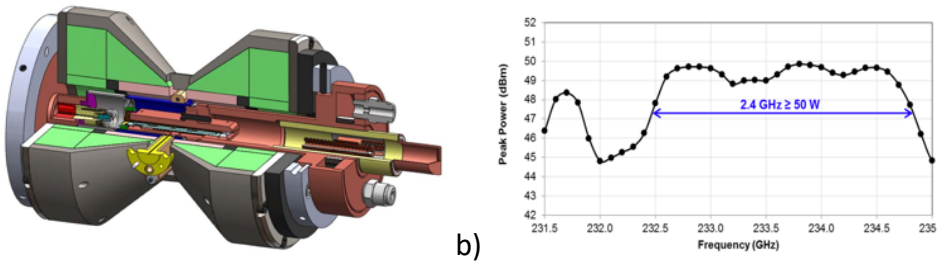

b)

Fig.29 Details of the a) FWG, b) cross-section of the TWT and c) output power as function of frequency. [123]

A FWG circuit realized by utilizing deep reactive ion etching (DRIE) and copper plating

(Fig. 29a) was used in a 233 GHz TWT (Fig. 29b) demonstrating an output power greater than 50 W over a 2.4 GHz instantaneous bandwidth (Fig.29c) [123].

Similar performance are reported for a 231.5–235 GHz FWG TWT (Fig.30a) providing a peak output power of 32 W (Fig.30 b) [15]. The TWT was designed to be integrated into an (Microwave Power Module) MPM for VISAR applications [14].

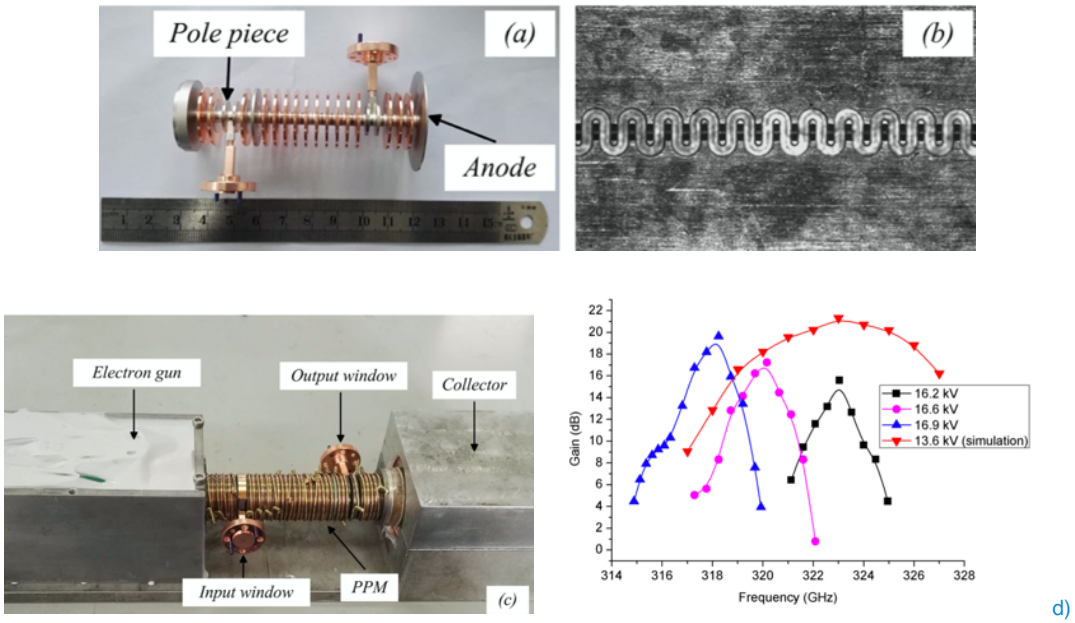

Fig. 31 a) Brazed high-frequency system including FWG, pole pieces, RF windows, and anode. (b) FWG half structure fabricated by the high-speed precision milling technology. (c) 0.32-THz FWG TWT. [124]

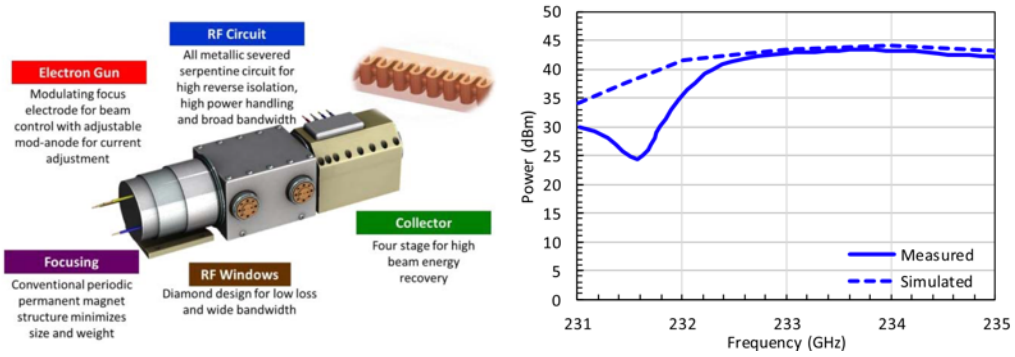

a) b)

Fig.30 a) G-band FWG TWT rendering and b) measured output power [15]

A 320 GHz FWG TWT has been fabricated with an FWG realized by high speed high precision milling machining (details in Fig. 31a,b). The TWT (Fig. 31c) achieved 130 mW of maximum output power and 19.6 dB gain at 318.24 GHz (Fig. 31d) [124].

A 0.670 THz Power Module based on an FWG TWT driven by a solid-state power amplifier (SSPA) has produced more than 100 mW with 21.5 dB gain in the 0.640-0.685

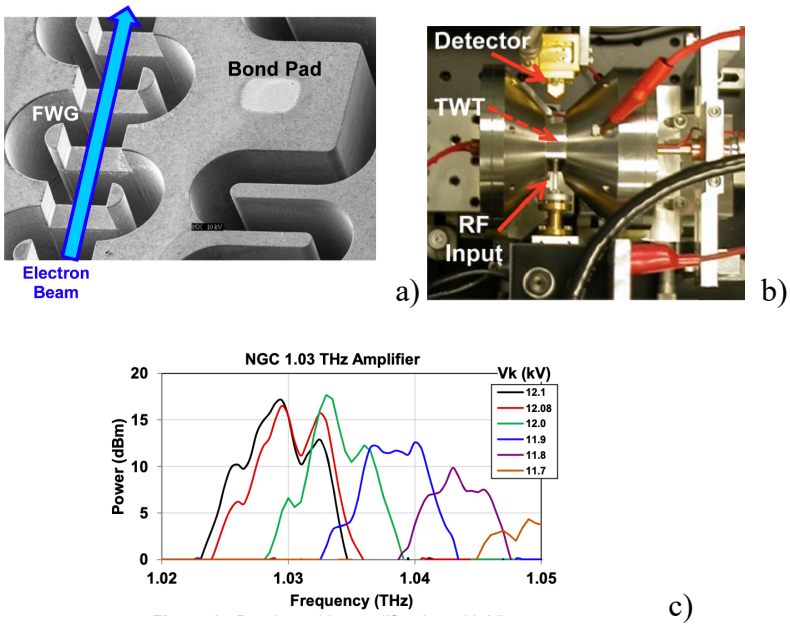

a) b) c)

Fig.32 a) SEM image of a FWG halve after Cu plating, prior to bonding, b) 1.03 THz TWT [21], c) output power measured at different beam voltage.

THz range in a bread-board demonstration. The TWT is based on a folded waveguide slow-wave circuit built by DRIE. [78]. An 850 GHz FWG vacuum tube demonstrated 50 mW of output power in the band 0.835-0.842 THz and 39.4 mW at 0.850 THz [23].
The 1 THz FWG TWT reported in [21] is the highest frequency TWT measured. It was built by a high precision OFHC- copper electroplated folded waveguide (FWG) made by 2-level, deep reactive-ion etching (DRIE) of silicon-on-insulator (SOI) wafers (Fig.32a). The waveguide dimensions are in the order of tens of microns. The TWT (Fig. 32b) demonstrated 29 mW power at 1.03 THz with 20 dB of saturated gain (Fig. 32c).

The magnetic focusing of the last three FWG TWTs described was provided by permanent magnet solenoid.

Finally, the development of such a wide range of FWG TWTs demonstrates the FWG as a very flexible SWS. Most of the prototypes presented were a first trial; further improvements are expected in the future.

Double Staggered waveguide

In early 2001, based on the previous analytic analysis of the rippled waveguide [125], the planar microfabricated sheet beam traveling-wave tube (TWT) amplifiers have been designed to satisfy the need for high-frequency, high-power sources of advanced radar and communication systems above 100 GHz, with peak powers of several hundred watts, and bandwidths of up to 10% [126]. As shown in the Fig. 33, this structure consists of a

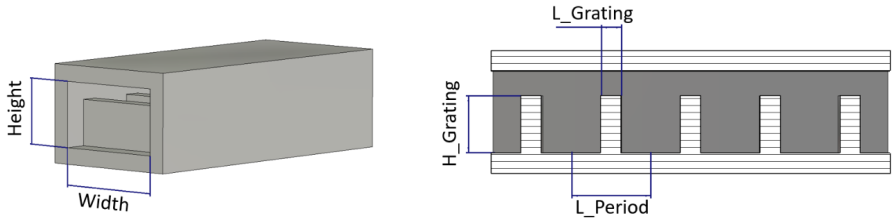

Fig. 33 Planar Grating SWS [126].

rectangular waveguide including a rectangular grating leading to EM wave diffraction. This SWS supports a sheet beam permitting the use of a high beam current with a low beam current density, due to the wide cross section. The sheet beam can be focused by a periodically cusped magnetic system [127]. In order to improve the beam-wave interaction efficiency by increasing the coupling impedance, a planar ridge waveguide was investigated Fig.34 (a) [126]. Further improvements were obtained by the double staggered grating (DSG) SWS, shown in Fig. 34 (b), in terms of ultra-wide operation frequency band [128]-[131].

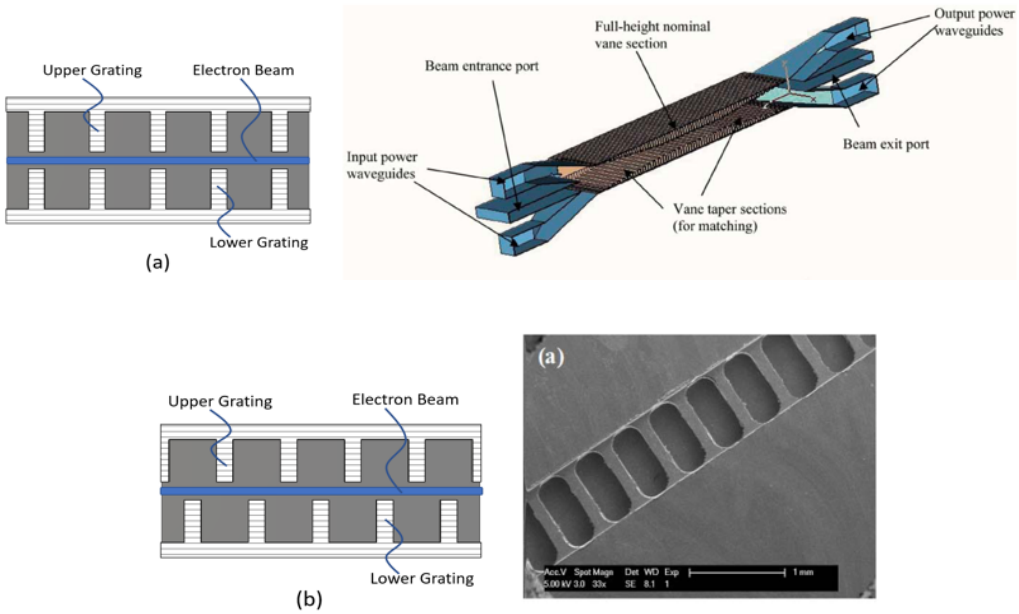

Fig. 34 a) Rectangular Grating Waveguide [125], b) double staggered waveguide

The DSG can be fabricated both by CNC milling and LIGA. A DSG was fabricated by LIGA using KRPM photoresist to operate in the frequency range 214 to 266 GHz [79]. The RF measurements demonstrated excellent RF transmission with insertion loss fluctuating between 5 to 10 dB and the return loss fluctuating by + 3 dB around 7.5 dB [80]. To improve the electrical behavior, the Nano-CNC milling has been used to manufacture the DSG [81]. The cold test results showed 5 dB insertion loss and -10 dB

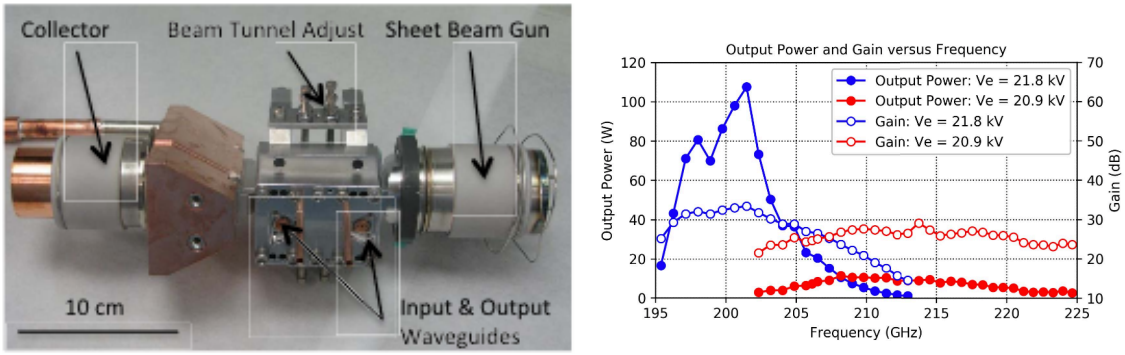

Fig. 35 a) 220 GHz DGS TWT, b) output power [81].

return loss in the 200 - 265 GHz range. A 220-GHz Sheet Beam TWT amplifier, employing a Nano-CNC DSG circuit (Fig. 35a), developed under the Defense Advanced Research Projects Agency (DARPA) HiFIVE program, provides more than 24 dB gain over the frequency range of 207–221 GHz, for 20.9 kV beam voltage (Fig. 35b). In the high-gain operation mode, with 21.8 kV beam voltage, over 30 dB of gain was measured over the frequency range of 197–202 GHz [82].

Double Corrugated Waveguide

The double corrugated waveguide (DCW) was conceived for the first 1 THz backward wave tube realized in the frame of the OPTHER project [132]. The challenge of the project, due to the short wavelength, was to find an SWS able to support a cylindrical beam and feasible by micromachining. The only available solution was the structure used in the carcinotron [43], but its low interaction property allows very low gain and power

The core of the DCW consists of two rows of parallel pillars in a rectangular waveguide. It was discovered that if two pillars are close to each other and have small cross-section, a quasi-round electric field is established between the two pillars (Fig. 36). The space between the two rows is the beam channel. The beam axis position needs to be optimized depending on the DCW size and frequency. The mode propagating in the DCW is a hybrid TE_{10}. Of great importance is the design of the coupler to provide the best match with the TE_{10} mode at the flanges. The DCW demonstrated up to 2 Ω interaction impedance up to 1 THz. This value permits a good interaction beam-wave at that frequency. The fabrication of the DCW (pillar dimensions 20 x 20 x 60 microns) was performed by deep-X-ray LIGA [64].

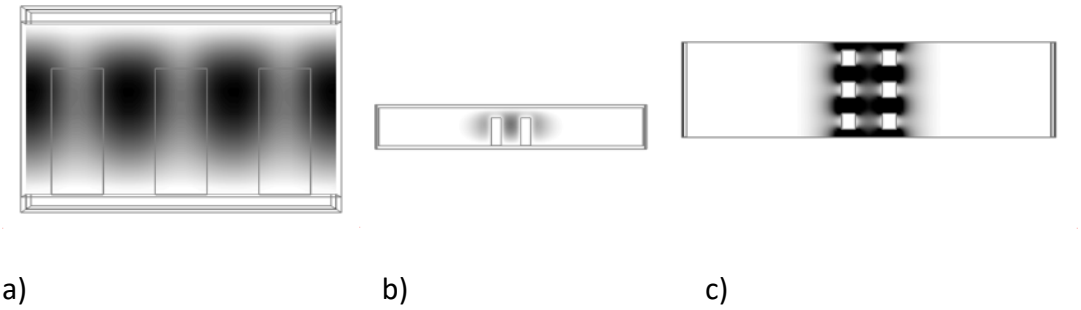

a) b) c)

Fig. 36 DCW Field distribution a) side, b) front, c) top

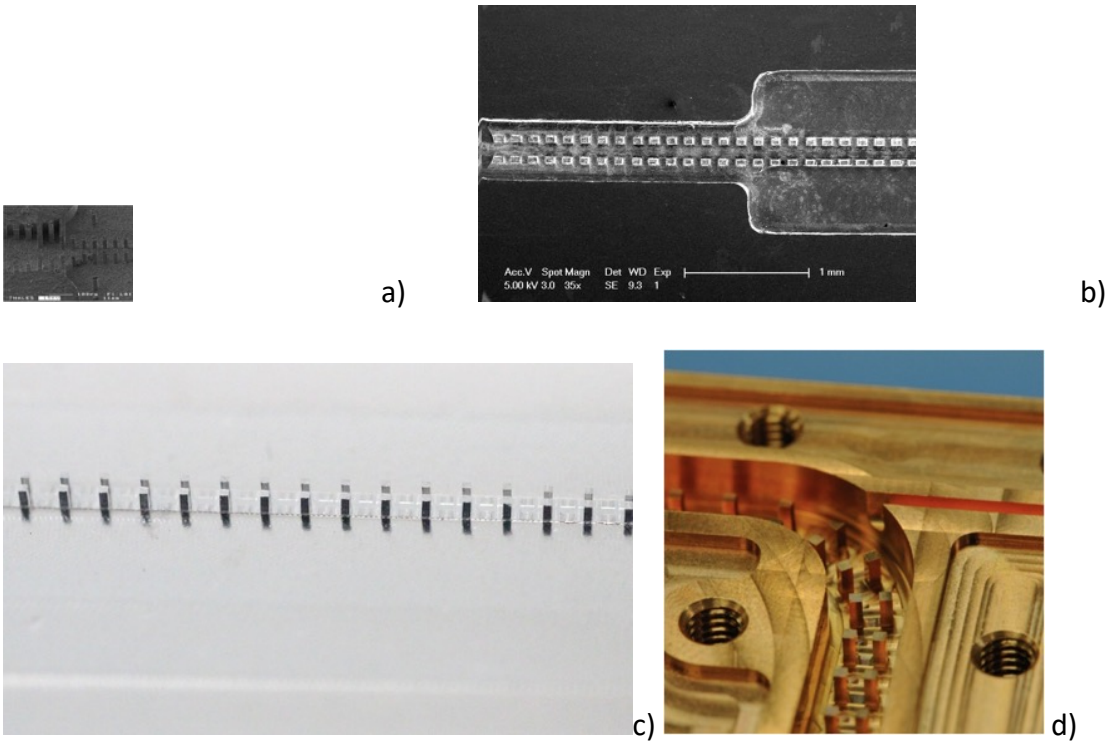

Fig. 37 DCW at different frequencies a) 1THz [64], b) 0.346 THz [13], c) 94 GHz , d) 34 GHz [133]

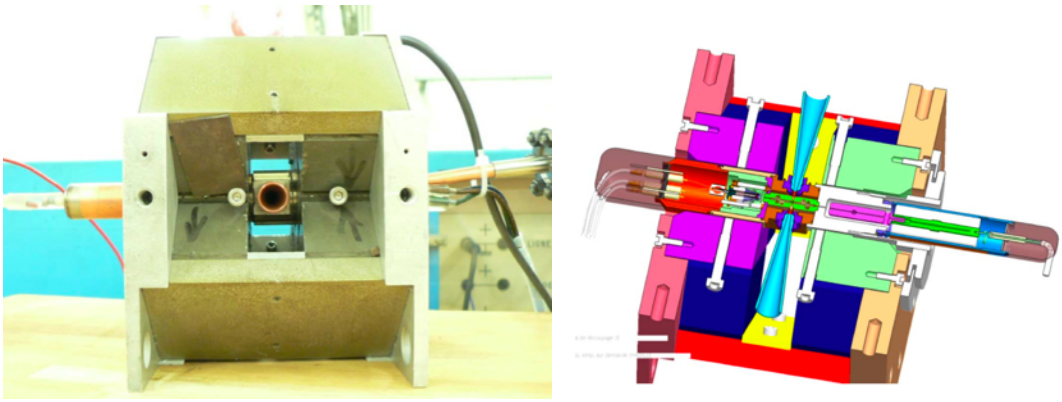

Fig. 38 1 THz Backward Wave Amplifier; a) realization, b) schematic [64].

The DCW was built for many different frequency bands, from 30 GHz to 1 THz by different micromachining processes, such as CNC milling [133][134], and UV LIGA [67] (Fig.37). In all the cases, it has demonstrated very good dispersion and interaction impedance. The flexibility of the DCW permitted the use of different coupler topologies depending on the fabrication process (e.g. LIGA does not permit the tapering of the height of pillars). A Backward Wave Amplifier at 1 THz was built by using the first 1 THz DCW realized by deep-Xray LIGA [64] (Fig.38).

A number of projects are in progress to implement the DCW in traveling wave tubes and backward wave oscillators at millimeter waves [135][136].

Conclusions

TWTs, and in general vacuum electronics devices at millimeter waves, are in a phase of rapid evolution from the traditional microwave helix TWTs to innovative topologies, born to overcome the fabrication challenges that the short wavelength at millimeter wave poses. This review paper has covered the major advancements in the field, including new fabrication processes and topologies and provided the fundamental background to appreciate the technological steps and the state of the art of millimeter waves and THz TWT. The road for a commercialization and wide use of millimeter wave TWT starts to be defined. Applications in many fields, such as wireless communications, plasma diagnostics, security, non-destructive product inspection, healthcare, will benefit of their high output power over a wide bandwidth above 100 GHz, so far not available. The relevant progress of the last years and the huge effort worldwide will bring substantial progress in year to come, revolutionizing the oldest electronic device technology.

References

[1] J. W. Gewartowski and H. A. Watson, Principles of Electron Tubes, *Van Nostrand*, 1965.

[2] J. Whitaker, Power Vacuum Tubes Handbook, *CRC Press*, 1999.

[3] R. J. Barker et al., Modern Microwave and Millimeter-Wave Power Electronics, *Wiley-IEEE Press*, April 2005.

[4] A. S. Gilmour, Klystrons, Traveling Wave Tubes, Magnetrons, Crossed-field Amplifiers, and Gyrotrons, *Artech House Microwave Library*, 2011.

[5] R. Carter, Microwave and RF Vacuum Electronic Power, *Cambridge University Press*, 2018.

[6] R. G. Symons and L. J. Murphy, Acute Changes In Thyroid Function Tests Following Ingestion Of Thyroxine, *Clinical Endocrinology*, 19: 539-546, 1983.

[7] D. Minenna et al, The Traveling-Wave Tube in the History of Telecommunication. *The European Physical Journal H*, vol. 44, issue 1, pp 1-36, 2019.

[8] R. Kompfner, The Traveling Wave Valve, *Wireless World*, 52(11): 369-372, 1946.

[9] R. Kompfner, The traveling wave tube as an amplifier at microwaves, *Proc. of the IRE*, 35(2): 124-127, 1947.

[10] R. Kompfner, The Invention of the Traveling-Wave Tube, *San Francisco Press*, 1964.

[11] Federici, J. F., B. Schulkin, F. Huang, D. Gary, R. Barat, F. Oliveira, and D. Zimdars, "THz imaging and sensing for security applications - Explosives, weapons and drugs," Semiconductor Science and Technology, Vol. 20, No. 7, S266-S280, 2005.

[12] Li, X., Huang, X., Mathisen, S., Letizia, R., Paoloni, C., "Design of 71-76 GHz Double-Corrugated Waveguide Traveling-Wave Tube for Satellite Downlink", in IEEE Transactions on Electron Devices. 65, 6, p. 2195-2200 6p. June 2018.

[13] Feng, J., Tang, Y., Gamzina, D., Li, X., Popovic, B., Gonzalez, M., Himes, L., Barchfeld, R., Li, H., Pan, P., Letizia, R., Paoloni, C., Luhmann Jr, N.C., "Fabrication of 0.346 THz BWO for Plasma Diagnostics", in IEEE Transactions on Electron Devices, 8 p. March 2018.

[14] Kim, R. Fan and F. Dominski, "ViSAR: A 235 GHz radar for airborne applications," 2018 IEEE Radar Conference (RadarConf18), Oklahoma City, OK, 2018, pp. 1549-1554.

[15] C. M. Armstrong et al., "A Compact Extremely High Frequency MPM Power Amplifier," in IEEE Transactions on Electron Devices, vol. 65, no. 6, pp. 2183-2188, June 2018. doi: 10.1109/TED.2018.2808327

[16] J. R. Pierce, "Theory of the beam-type traveling-wave tube," *Proc. IRE*, vol. 35, pp. 111–123, Feb. 1947.

[17] J. F. Gittins, Power Travelling-wave Tubes, *American Elsevier Publishing Company*, 1965 .

[18] A. Baig et al., 0.22 THz wideband sheet electron beam traveling wave tube amplifier: Cold test measurements and beam wave interaction analysis, *Physics of Plasmas*, 19, 093110, 2012 .

[19] A. Baig et al., Design, Fabrication and RF Testing of Near-THz Sheet Beam, *Terahertz Science and Technology*, Vol.4, No.4, December 2011.

[20] C. Paoloni and M. Mineo, 0.22 THz TWT based on the Double Corrugated Waveguide, *IEEE International Vacuum Electronics Conference*, 22-24 April 2014 .

[21] J. C. Tucek et al., Operation of a compact 1.03 THz power amplifier*, IEEE International Vacuum Electronics Conference 2016*

[22] J. C. Tucek et al., 0.850 THz vacuum electronic power amplifier, *IEEE International Vacuum Electronics Conference 2014*

[23] M. A. Basten *et al*. 0.850 THz Vacuum Electronic Power Amplifier,' *Vacuum Electronics Conference (IVEC), 2012 IEEE Thirteenth International, 2012*.

[24] H. Heffner, Analysis of the Backward-Wave Traveling-Wave Tube, *Proc.of IRE*, pp. 930-937. June 1954.

[25] H. R. Johnson, Backward-Wave Oscillators, *Proc.of IRE*, pp. 684-697, June 1955.

[26] R. W. Grow and D. A. Watkins, Backward Wave Oscillator Efficiency, *Proc. of the IRE*, pp. 848-856, July 1955.

[27] A. Karp, Backward-Wave Oscillator Experiments at 100 to 200 Kilomegacycles, *Proc. of the I.R.E.*, Vol. 45, pp. 496-503, 1957.

[28] S. F. Paik, Design Formulas for Helix Dispersion Shaping, *IEEE Trans on Electron Devices*, vol. 16, no. 12, Dec. 1969.

[29] Z. J. Zhu and C. L. Wei, Simulation Modeling On Dispersion Shaping And Harmonic Suppression In Helix Twt from 2 Ghz to 6 Ghz, *Progress In Electromagnetics Research C*, Vol. 28, 181–193, 2012.

[30] C. R. Smith, C. M. Armstrong, and J. Duthie, The Microwave Power Module: A Versatile RF Building Block for High-Power Transmitters, *Proceedings of The IEEE*, vol. 87, no. 5, MAY 1999.

[31] A. R. Jung, 10 kW and Up, from a Helix TWT?, *Proc. of International Electron Devices Meeting*, 1978.

[32] C. E. Hobrecht, Resonant loss for helix traveling wave tubes, *Proc. of International Electron Devices Meeting*, 1977.

[33] C. K. Chong et al., Development of high-power Ka-band and Q-band helix-TWTs, *IEEE Trans. Electron Devices*, vol. 52, no. 5, pp. 653–659, May 2005.

[34] C. K. Chong, J. W. Forster, D. A. Layman, R. J. Stolz, and X. Zhai, Ka-band satellite uplink high-power helix TWTs: Output power evolution at L-3 ETI, *International Electron Devices Conference* 2010, pp. 53–54, May 2010.

[35] C. K. Chong, D. A. Layman, R. J. Stolz, B. Levush, and J. Pasour, Development of high-power K/Ka-band helix TWT, *International Electron Devices Conference 2012* , pp. 119–120, Apr. 2012.

[36] R. H. LeBorgne et al., Development of an 800W Ka-Band, Ring-Bar TWT, *International Technical Digest on Electron Devices Conference 1990,* Dec. 1990.

[37] D. Wilson, A Millimeter-Wave Tunneladder TWT Final Report, NASA Contract Report 182183, Oct. 1988.

[38] H. G. Kosmahl and R. W. Palmer, Harmonic Analysis Approach to the ”TunneLadder“: A Modified Karp Circuit for Millimeter-Wave TWTA’s, *IEEE Trans. Electron Device*, Vol. 29, No. 5, May 1982.

[39] A. Karp, Traveling wave tube experiments at millimeter wavelength with a new, easily built, space harmonic circuit. *Proc. of the IRE*. 43, 41-46, 1956.

[40] A. Karp, Millimeter Wave Valves, *Fortschritte der Hochfrequenztechnik, Vol. 5., Academlc Press MBH, Frankfurt/Main*, pp. 73-128, 1960.

[41] R. A. Craig and Y. Hiramatsu, A Pulsed 10 Megawatt Travelling-Wave Tube Amplifier *Proceedings of the International Congress on Microwave Tubes, Munich, Germany*, pp.94-97, 1960.

[42] M. Chodorow, A. F. Pearce, and D. K. Winslow, The Centipede High Power Traveling Wave Tube. *Microwave Laboratory, Report No. 695 Stanford University*, 1960.

[43] P. Palluel and A. K. Goldberger, The 0-Type Carcinotron Tube, *Proc. of the I.R.E*, pp. 333-345. March 1956.

[44] G.O. Chalk, and P.M. Chalmers, A 500 KW Travelling Wave Tube for X-band, *6th Int. Conf. on Microwave and Optical Generation and Amplification*, *Cambridge, England*, pp. 54-58, 1966.

[45] T. Roumbanis, J. Needle, and D.K. Winslow, A Megawatt X-band TWT Amplifier with 18% Bandwidth, *Proc. of the High-Power Microwave Symposium, 1 The Hexagon, Fort Monmouth, New Jersey*, pp. 114-129, 1962.

[46] G. Kantorowicz and P. Palluel, Backward Wave Oscillators, *Infrared and Millimeter Waves by K.J. Button, Academic Press (New York),* 1979.

[47] D. C. Forster, High Power Millimeter Wave Sources, *Advances in Microwaves*, pp. 301-346, 1968.

[48] F. Lewen et al, Phase locked backward wave oscillator pulsed beam spectrometer in the submillimeter wave range, *Review of Scientific Instruments*, vol. 69, 32, 1998.

[49] A. van Ardenne, E. E. M. Woestenburg, and L. J. van der Ree, 350-GHz phase/frequency locked loop for use with a carcinotron backward wave oscillator, *Review of Scientific Instruments*, vol. 57, 2547, 1986.

[50] A. H. F. van Vliet et al.,, A low noise heterodyne receiver for astronomical observations operating around 0.63 mm wavelength, *International Journal of lnfrared and Millimeter Waves*, Vol. 3, No. 6, 1982

[51] N. J. Keen et al., Low-noise 460 GHz waveguide Schottky mixer radiometer for radioastronomy, *Electronics Letters*, Vol.22 No. 7, 27 March 1986

[52] N. C. Luhmann, Jr., et al., Millimeter and Submillimeter Wave Diagnostic Systems for Contemporary Fusion Experiments, in Diagnostics for Contemporary Fusion Experiments, *D.K.k. P.E.* Stott, G. Gorini and E. Sindoni, Editor, SIF: Bologna. p. 135-17, 1991

[53] H. J. Hartfuß and T. Geist, Fusion Plasma Diagnostics with Mm Waves. Weinheim, Germany: Wiley-VCH Verlag GmbH & Co. KGaA, 2013. [Online]. Available: http://www.wiley-vch.de

[54] H. J. Hartfuss, RF techniques in plasma diagnostics, *Plasma Phys. Controlled Fusion*, vol. 40, no. 8A, pp. A231–A250, 1998.

[55] H. J. Hartfuss, T. Geist, and M. Hirsch, Heterodyne methods in millimetre wave plasma diagnostics with applications to ECE, interferometry and reflectometry, *Plasma Phys. Controlled Fusion*, vol. 39, no. 11, pp. 1693–1769, 1997.

[56] N. C. Luhmann, Jr. et al, Microwave diagnostics, *Fusion Sci. Technol*., vol. 53, no. 2, pp. 335–396, Apr. 2008.

[57] N. C. Luhmann, Jr. and W. A. Peebles, Instrumentation for magnetically confined fusion plasma diagnostics, *Review of Scientific Instruments*, vol. 55, 279, 1984.

[58] G. Kozlov and A. Volkov, Coherent Source Submillimeter Wave, Spectroscopy, *Millimeter and Submillimeter Wave Spectroscopy of Solids. Topics in Applied Physics*. vol. 74, 1998.

[59] Ph. Guidee, L. Teyssier, A 850 - 1000 GHz Backward-Wave Oscillator for Advanced Applications, *Proc. SPIE 0598, Instrumentation for Submillimeter Spectroscopy*, April 1986.

[60] L. Teyssier and R. Gerber, A Wideband, High-Power 0-Type Carcinotron Operating Near 94 GHz*. Proc. of IEDM, Washington*, 1987.

[61] A. A. Borisov et al., The Development of Vacuum Microwave Devices in Istok, *2011 IEEE International Vacuum Electronics Conference (IVEC*), 2011.

[62] R. L. Ives, "Microfabrication of high-frequency vacuum electron devices," IEEE Trans. Plasma Sci., vol. 32, no. 3, pp. 1277-1291, Jun. 2004.

[63] Genolet, G.; Lorenz, H. UV-LIGA: From Development to Commercialization. Micromachines 2014, 5, 486-495.

[64] C. Paoloni et al., "Design and Realization Aspects of 1-THz Cascade Backward Wave Amplifier Based on Double Corrugated Waveguide," in IEEE Transactions on Electron Devices, vol. 60, no. 3, pp. 1236-1243, March 2013.

[65] C. Tucek *et al*, 'Operation of a compact 1.03 THz power amplifier,*' Vacuum Electronics Conference (IVEC), 2016 IEEE Thirteenth International*, 2016.

[66] O. V. Makarova, R. Divan, J. Tucek, K. Kreischer and C. Tang, "Fabrication of solid copper two-level waveguide circuits for a THz radar system by UV lithography," 2016 IEEE International Vacuum Electronics Conference (IVEC), Monterey, CA, 2016, pp. 1-2.

[67] Malek Abadi, S.A. & Paoloni, C., "UV-LIGA microfabrication process for sub-terahertz waveguides utilizing multiple layered SU-8 photoresist" in Journal of Micromechanics and Microengineering. 26, 9, 8 p., 095010. July 2016.

[68] C. D. Joye et al., 'Microfabrication of wideband distributed beam amplifiers at 220 GHz,' *in Vacuum Electronics Conference (IVEC), 2011 IEEE International*, pp. 343-344, 2011.

[69] D. J. Colin et al., 'Microfabrication of fine electron beam tunnels using UV-LIGA and embedded polymer monofilaments for vacuum electron devices,' Journal of Micromechanics and Microengineering, vol. 22, p. 015010, 2012.

[70] C. D. Joye, et al., "UV-LIGA and DRIE grating microfabrication and testing for sheet beam amplifiers at 220 GHz," in Infrared Millimeter and Terahertz Waves (IRMMW-THz), 2010 35th International Conference on, 2010, pp. 1-2.

[71] C. D. Joye, 'UV-LIGA Microfabrication of 220 GHz sheet beam amplifier gratings with SU-8 photoresists,' Journal of Micromechanical Microengineering, vol. 20, p. 125016, 2010.

[72] C. D. Joye *et al.*, "Demonstration of a high power, wideband 220-GHz traveling wave amplifier fabricated by UV-LIGA," *IEEE Trans. Electron Devices*, vol. 61, no. 6, pp. 1672–1678, Jun. 2014.

[73] M. Yoshida et al., "Development activity of Terahertz amplifiers with FWG-TWTs," 2016 IEEE International Vacuum Electronics Conference (IVEC), Monterey, CA, 2016

[74] Y. Hou *et al.*, 'A novel ridge-vane-loaded folded-waveguide slow wave structure for 0.22-THz traveling-wave tube,' *IEEE Trans. Electron Devices*, vol. 60, no. 3, pp. 1228–1235, Mar. 2013.

[75] Y. Hou *et al.*, 'Equivalent circuit analysis of ridge-loaded folded waveguide slow-wave structures for millimeter-wave traveling-wave tubes,' *Prog. Electromagnetic. Res.*, vol. 129, pp. 215–229, 2012.

[76] X. Xu *et al*, 'Sine Waveguide for 0.22-THz Traveling-Wave Tube,' *IEEE Electron Device Letters*, vol. 32, no.8, pp. 1152-1154, 2011.

[77] J. C. Tucek *et al*, '220 GHz power amplifier development at Northrop Grumman,*' Vacuum Electronics Conference (IVEC), 2012 IEEE Thirteenth International*, pp. 553 – 554, 2012.

[78] J. C. Tucek *et al*, 'A 100 mW, 0.670 THz Power Module,*' Vacuum Electronics Conference (IVEC), 2012 IEEE Thirteenth International*, pp. 553 – 554, 2012.

[79] A. Baig *et al*., 'Design, Fabrication and RF Testing of Near-THz Sheet Beam TWTA,' Special Issue (Invited Paper), *Terahertz Science and Technology*, vol. 4, Dec 2011.

[80] A. Baig *et al*., 'Experimental characterization of LIGA fabricated 0.22 THz TWT circuits,' *IEEE International Vacuum Electronics Conference (IVEC)*, pp. 275-276, 2011.

[81] R. A. G. Barchfeld *et al*, 'Microfabrication of Terahertz Vacuum Electronics Devices,' *American Society for Precision Engineers Conference,* 2011.

[82] A. Baig *et al*. 'Performance of a Nano-CNC Machined 220-GHz Traveling Wave Tube Amplifier,' *IEEE Transactions on Electron Devices*, vol. 64, no. 5, pp. 2390-2397, 2017.

[83] D. Gamzina et al., "Nano-CNC Machining of Sub-THz Vacuum Electron Devices," in IEEE Transactions on Electron Devices, vol. 63, no. 10, pp. 4067-4073, Oct. 2016. doi: 10.1109/TED.2016.2594027.

[84] F. André et al., "Technology, Assembly, and Test of a W-Band Traveling Wave Tube for New 5G High-Capacity Networks," in IEEE Transactions on Electron Devices, vol. 67, no. 7, pp. 2919-2924, July 2020, doi: 10.1109/TED.2020.2993243.

[85] C. Paoloni, V. Krozer, F. Magne, Q. T. Le, R. Basu, J. Rao, R. Letizia, E. Limiti, M. Marilier, G. Ulisse, A. Ramirez, B. Vidal, H. Yacob. "D-band Point to Multi-Point Deployment with G-Band Transport," at European Conference on Networks and Communications 2020

[86] J. W. Elmer, J. Klingmann, and K. Van Bibber, Diffusion bonding and brazing of high purity copper for linear collider accelerator structures, PHYSICAL REVIEW SPECIAL TOPICS - ACCELERATORS AND BEAMS, VOLUME 4, 053502 (2001)

[87] M. Field et al., "Development of a 100-W 200-GHz High Bandwidth mm-Wave Amplifier," in IEEE Transactions on Electron Devices, vol. 65, no. 6, pp. 2122-2128, June 2018. doi: 10.1109/TED.2018.2790411

[88] B. E. Carlsten et al, 'Stability of an emittance-dominated sheet-electron beam in planar wiggler and periodic permanent magnet structures with natural focusing', Phys. Rev. ST Accel. Beams, Vol. 8, No. 062001, pp. 1-14, November 2005

[89] John H. Booske, Brian D. McVey and Thomas M. Antonsen Jr., 'Stability and confinement of nonrelativistic sheet electron beams with periodic cusped magnetic focusing', J. Appl. Phys. Vol. 73, No. 9, pp. 4140-4155, May 1993

[90] J. H. Booske et al, 'Periodic magnetic focusing of sheet electron beams', Phys. Plasmas, Vol. 1, No. 5, pp. 1714-1720, May 1994

[91] Jian-Xun Wang et al, 'Electron beam transport analysis of W-band sheet beam klystron', Phys. Plasmas, Vol. 17, No. 043111, September 2010

[92] Y. Zheng, D. Gamzina, L. Himes, M. Gonzalez and N. C. Luhmann, "Design and Analysis of the Staggered Double Grating Slow Wave Circuit for 263 GHz Sheet Beam TWT," in IEEE Transactions on Terahertz Science and Technology, vol. 10, no. 4, pp. 411-418, July 2020, doi: 10.1109/TTHZ.2020.2995826.

[93] Pershing, et. al, "Demonstration of a Wideband 10-kW Ka-Band Sheet Beam TWT Amplifier," IEEE Transactions on Electron Devices 61(6):1637-1642.

[94] [28] F. Shen *et al.*, "A novel V-shaped microstrip meander-line slow-wave structure for W-band MMPM," *IEEE Trans. Plasma Sci.*, vol. 40, no. 2, pp. 463–469, Feb. 2012. doi: 10.1109/tps.2011.2175252.

[95] F. Shen *et al.*, "Symmetric double V-shaped microstrip meander- line slow-wave structure for W-band traveling-wave tube," *IEEE Trans. Electron Devices*, vol. 59, no. 5, pp. 1551–1557, May 2012. doi: 10.1109/Ted.2012.2188635.

[96] X. Li *et al.*, "Study on phase velocity tapered microstrip angular log- periodic meander line travelling wave tube," *IET Microw., Antennas Propag.*, vol. 10, pp. 902–907, Jun. 2016. doi: 10.1049/iet-map.2015. 0520.

[97] S. Wang, Y. Hou, Y. Wei, Z. Duan, and Y. Gong, "Study on 800 V traveling-wave tube," *High Power Laser Particle Beams*, vol. 25, no. 7, pp. 1613–1614, 2013. doi: 10.3788/HPLPB20132507.1613.

[98] S. Wang *et al.*, "Study of a log-periodic slow wave structure for Ka-band radial sheet beam traveling wave tube," *IEEE Trans. Plasma Sci.*, vol. 41, no. 8, pp. 2277–2282, Aug. 2013. doi: 10.1109/TPS.2013.2271639.

[99] S. Wang, Y. Gong, Z. Wang, Y. Wei, Z. Duan, and J. Feng, "Study of the symmetrical microstrip angular log-periodic meander-line traveling- wave tube," *IEEE Trans. Plasma Sci.*, vol. 44, no. 9, pp. 1787–1793, Sep. 2016. doi: 10.1109/TPS.2016.2598614.

[100] H. Wang *et al.*, “Study of a miniaturized dual-beam TWT with planar dielectric-rods-support uniform metallic meander line,” *Phys. Plasmas*, vol. 25, May 2018, Art. no. 063113. doi: 10.1063/1.5023776.

[101] X. Li *et al.*, “Study on radial sheet beam electron optical system for miniature low-voltage traveling-wave tube,” *IEEE Trans. Electron Devices*, vol. 64, no. 8, pp. 3405–3412, Aug. 2017. doi: 10.1109/TED. 2017.2711616.

[102] C. Zhao, S. Aditya and C. Chua, "Analysis of Coupled Planar Helices with Straight-Edge Connections for Application in Millimeter-Wave TWTs," in IEEE Transactions on Electron Devices, vol. 60, no. 3, pp. 1244-1250, March 2013 doi: 10.1109/TED.2013.2241437

[103] K. T. Nguyen et al., "Design Methodology and Experimental Verification of Serpentine/Folded-Waveguide TWTs," in IEEE Transactions on Electron Devices, vol. 61, no. 6, pp. 1679-1686, June 2014, doi: 10.1109/TED.2014.2303711.

[104] X. Zhang *et al.*, “Design and experimental study of 250-W *W*-band pulsed TWT With 8-GHz bandwidth,” *IEEE Electron Device*, vol. 64, no. 12, pp. 5151–5156, Dec. 2017.

[105] Y. Wei *et al.*, “Novel W-band ridge-loaded folded waveguide traveling wave tube,” *IEEE Electron Device Lett.*, vol. 35, no. 10, pp. 1058–1060, Oct. 2014.

[106] [18] Y. Hou *et al.*, “A novel ridge-vane-loaded folded-waveguide slow- wave structure for 0.22-THz traveling-wave tube,” *IEEE Trans. Electron Devices*, vol. 60, no. 3, pp. 1228–1235, Mar. 2013. doi: 10.1109/ TED.2013.2238941.

[107] Y. Hou *et al.*, “Equivalent circuit analysis of ridge-loaded folded- waveguide slow-wave structures for millimeter-wave traveling-wave tubes,” *Prog. Electromagn. Res.*, vol. 129, pp. 215–229, 2012. doi: 10.2528/PIER12042602.

[108] H. Gong, Y. Gong, T. Tang, J. Xu, and W.-X. Wang, “Experimental investigation of a high-power Ka-band folded waveguide traveling-wave tube,” *IEEE Trans. Electron Devices*, vol. 58, no. 7, pp. 2159–2163, Jul. 2011. doi: 10.1109/TED.2011.2148119. IEEE TRANSACTIONS ON PLASMA SCIENCE, VOL. 47, NO. 5, MAY 2019

[109] H. Gong *et al.*, “A high efficiency Q-band folded waveguide traveling- wave tube,” in *Proc. IEEE Int. Vac. Electron. Conf.*, Monterey, CA, USA, Apr. 2014, pp. 127–128. doi: 10.1109/IVEC.2014.6857522.

[110] M. Liao *et al.*, “A V-band folded waveguide TWT,” in *Proc. IEEE Int. Vac. Electron. Conf.*, Beijing, China, Apr. 2015, pp. 1–2. doi: 10.1109/ IVEC.2015.7223937.

[111] J. Feng et al., "Development of W-band Folded Waveguide Pulsed TWTs," in IEEE Transactions on Electron Devices, vol. 61, no. 6, pp. 1721-1725, June 2014

[112] [X. Xu *et al.*, “Sine waveguide for 0.22-THz traveling-wave tube,” *IEEE Electron Device Lett.*, vol. 32, no. 8, pp. 1152–1154, Aug. 2011. doi: 10.1109/led.2011.2158060.

[113] L. Zhang *et al.*, “A ridge-loaded sine waveguide for *G*-band traveling- wave tube,” *IEEE Trans. Plasma Sci.*, vol. 44, no. 11, pp. 2832–2837, Nov. 2016. doi: 10.1109/Tps.2016.2605161.

[114] S. Fang *et al.*, “Study on W-band sheet-beam traveling-wave tube based on flat-roofed sine waveguide,” *AIP Adv.*, vol. 8, May 2018, Art. no. 055116. doi: 10.1063/1.5028300.

[115] X. Lei *et al.*, “Full-wave analysis of the high frequency characteristics of the sine waveguide slow-wave structure,” *AIP Adv.*, vol. 7, Aug. 2017, Art. no. 085111. doi: 10.1063/1.4997329.

[116] X. Lei *et al.*, “Linear analysis of traveling sheet electron beam in sine waveguide tubes,” *J. Appl. Phys.*, vol. 124, Sep. 2018, Art. no. 133301. doi: 10.1063/1.5025373.

[117] Z. Wang *et al.*, “Development of a 140-GHz folded-waveguide traveling wave tube in a relatively larger circular electron beam tunnel,” *J. Electromagn. Waves Appl.*, vol. 31, no. 17, pp. 1914–1923, 2017.

[118] P. Pan *et al.*, “Development of 220 GHz and 340 GHz TWTs,” in *Proc. IEEE 9th UK-Eur.-China Workshop Millimetre Waves THz. Tech- nol. (UCMMT)*, Qingdao, China, Sep. 2016, pp. 39–41. doi: 10.1109/ UCMMT.2016.7873954.

[119] Lei Wenqiang, Jiang Yi, Zhou Quanfeng, Hu Peng, Hu Linlin, Yan Lei, Chen Hongbin, “Development of D-band Continuous-wave Folded Waveguide Traveling-Wave Tube”, *IEEE International Vacuum Electronics Conference (IVEC),* 2015.

[120] H. Li, J. Cai, Y. Du, X. Li, and J. Feng, “UV-LIGA microfabrication for high frequency structures of a Y-band TWT 2nd harmonic amplifier,” in *Proc. IEEE Int. Vac. Electron. Conf. (IVEC)*, Apr. 2015, pp. 1–2.

[121] Q. Zhou et al., "Development of a 0.22THz folded waveguide travelling wave tube," 2015 IEEE International Vacuum Electronics Conference (IVEC), Beijing, 2015, pp. 1-2, doi: 10.1109/IVEC.2015.7223971.

[122] H. R. Gong *et al.*, “Third-harmonic traveling-wave tube multiplier- amplifier,” *IEEE Trans. Electron Devices*, vol. 65, no. 6, pp. 2189–2194, Jun. 2 018. doi: 10.1109/Ted.2017.2785661.

[123] M. A. Basten, J. C. Tucek, D. A. Gallagher, and K. E. Kreischer, “233 GHz high Power amplifier development at Northrop Grumman,” in *Proc. IEEE Int. Vacuum Electron. Conf. (IVEC)*, Apr. 2016, pp. 1–2.

[124] P. Hu *et al.*, “Development of a 0.32-THz folded waveguide traveling wave tube,” *IEEE Trans. Electron Devices*, vol. 65, no. 6, pp. 2164–2169, Jun. 2018. doi: 10.1109/TED.2017.2787682.

[125]] B. E. Carlsten et al. ‘Pierce gain analysis for a sheet beam in a rippled waveguide traveling wave tube,’ Phys. Plasmas, vol. 8, pp. 4585–4591, Oct. 2001.

[126] B. E. Carlsten *et al*. ‘Technology development for a mm-wave sheet-beam traveling-wave tube,’ *IEEE Transactions on Plasma Science*, vol. 33, no. 1, pp. 85-93, 2005.

[127] M. A. Basten and J. H. Booske, “Two-plane Focusing of High Space Charge Sheet Electron Beams using Periodically Cusped Magnetic Fields”, J. Appl. Phys., vol. 85, no. 9, pp. 6313-6322, May 1999.

[128] Y. M. Shin and L. R. Barnett, ‘Intense wideband terahertz amplification using phase shifted periodic electron-plasmon coupling,’ *Appl. Phys. Lett.,* vol. 92, no. 9, pp. 091501-1–091501-3, Mar. 2008.

[129] https://patents.google.com/patent/US7952287B2/en

[130] Y. Zhang *et al.*, “A high-power single rectangular grating sheet electron beam traveling-wave tube,” *IEEE Trans. Electron Devices*, vol. 63, no. 8, pp. 3262–3269, Aug. 2016. doi: 10.1109/ted.2016.2576464.

[131] X. Shi *et al.*, “Theoretical and experimental research on a novel small tunable PCM system in staggered double vane TWT,” *IEEE Trans. Electron Devices*, vol. 62, no. 12, pp. 4258–4264, Dec. 2015. doi: 10.1109/Ted.2015.2483538.

[132] M. Mineo and C. Paoloni, “Double Corrugation Rectangular Waveguide Slow-wave Structure for THz Vacuum Devices”, IEEE Trans. on Electron Devices. Vol.57, N.11, pp.3169-3175, November 2010.

[133] Paoloni, C.; Mineo, M.; Henry, M.; Huggard, P.G., "Double Corrugated Waveguide for Ka-Band Traveling Wave Tube," in Electron Devices, IEEE Trans. on , vol. 62, no., pp.3851 – 3856.

[134] C. Paoloni, V. Krozer, F. Magne, Q. T. Le, R. Basu, J. Rao, R. Letizia, E. Limiti, M. Marilier, G. Ulisse, A. Ramirez, B. Vidal, H. Yacob. “D-band Point to Multi-Point Deployment with G-Band Transport,” at European Conference on Networks and Communications 2020

[135] R.Basu, L. R. Billa, R. Letizia, C. Paoloni, “Design of sub-THz traveling wave tubes for high data rate long range wireless links”, *2018 Semicond. Sci. Technol. 33* 124009

[136] R.Basu, L. R. Billa, R. Letizia, C. Paoloni, “Design of D-band Double Corrugated Waveguide TWT for Wireless Communications “, *Proc. IEEE 20th Int. Vac. Electron. Conf.*, Busan, South Kores, April. 2019